

RESEARCH ARTICLE

An endless summer: 2018 heat episodes in Europe in the context of secular temperature variability and change

Andreas Hoy¹  | Stephanie Hänsel^{1,2} | Maurizio Maugeri³

¹TU Bergakademie Freiberg,
Interdisciplinary Environmental Research
Center, Freiberg, Germany

²Department Hydrometeorology,
Deutscher Wetterdienst, Section Climate
and Environment, Offenbach, Germany

³Department of Environmental Science
and Policy, Università degli Studi di
Milano, Milan, Italy

Correspondence

Andreas Hoy, TU Bergakademie Freiberg,
Interdisciplinary Environmental Research
Center, Brennhausgasse 14, 09599
Freiberg, Germany.
Email: andreas.hoy@ioez.tu-freiberg.de

Abstract

The year 2018 was affected by very long-lasting, stable summer conditions in vast parts of Europe, in many regions already starting in April and lasting until October. We investigate the thermal characteristics of this year in a secular time perspective, using a spatially well-distributed dataset of 67 European stations (west of $\sim 30^\circ\text{E}$) with daily long-term air temperature observations. Our dataset comprises many of the longest and most reliable (homogenous) temperature measurements available in Europe, mainly starting already in the 19th or rarely even 18th century. Individual time series length is considered to analyse the summer 2018 temperatures into a more than two-century time perspective, while European time series are presented for the period 1855–2018 and records of five European regions are considered from 1881 onwards. The extreme long duration of the 2018 summer most clearly manifested itself in pronounced new continental maxima of summer half year (April–September) temperature averages and the number of days with maximum temperatures ≥ 20 and $\geq 25^\circ\text{C}$. Furthermore, those indices reached new local maxima at about half of our investigated stations. Records of other temperature indices, rather representing intense heat conditions, were particularly broken in the extended Baltic Sea region, supported by distinct and long-lasting anticyclonic conditions in this area. However, the extreme summer of 2003 still dominates the ranking of most of these indices on the continental level, even though it is now generally closely followed by summer 2018. We show that long-term variations of teleconnection indices and the Atlantic Multidecadal Oscillation, as well as seasonal and anthropogenic effects, supported both the recent hot summers and the extreme summer of 2018.

KEYWORDS

AMO, atmospheric circulation, daily climate indices, heat waves, homogeneity, instrumental observations, teleconnection indices

This is an open access article under the terms of the Creative Commons Attribution License, which permits use, distribution and reproduction in any medium, provided the original work is properly cited.

© 2020 The Authors. International Journal of Climatology published by John Wiley & Sons Ltd on behalf of the Royal Meteorological Society.

1 | INTRODUCTION

The summer half year (SHY) of 2018 was characterized by unusually early, long lasting, very persistent and regionally record-breaking heat conditions, coupled with a pronounced precipitation deficit and sunshine surplus in large areas of Europe. According national reports include, among others, Sweden (SHMI, 2018), Finland (FMI, 2018), Estonia (EMHI, 2018), Great Britain (MetOffice, 2018), The Netherlands (KNMI, 2018), Germany (DWD, 2018a, 2018b), Switzerland (MeteoSwiss, 2018), Austria (ZAMG, 2018) and Italy (ISPRA, 2018). Expectably, severe societal and environmental impacts were observed. They included unusual and wide-spread forest fires in Scandinavia, especially Sweden (Krisinformation, 2018), where NATO assistance was necessary to fight and contain the fires (NATO, 2018). Record-low river levels and very high water temperatures were witnessed in many areas, for example, Switzerland (BAFU, 2018) and Germany (BfG, 2019). Low soil moisture conditions triggered intense vegetation responses, like early leaf fall or even dying of otherwise healthy trees (BMEL, 2019). It also negatively affected crop harvests, which were below average in most of Europe (JRC, 2018) – for instance in Germany especially for grain and rapeseed (BMEL, 2018).

2018 continues the series of very hot summers of recent years, which – since the previously unprecedented summer of 2003 (Luterbacher *et al.*, 2004) – strongly accumulated in Europe (e.g., Christidis *et al.*, 2015; Russo *et al.*, 2015; Dong *et al.*, 2017; Manning *et al.*, 2019). The 2003 summer was up to five degrees warmer than (1961–1990) average conditions in the greater alpine area, with large anomalies in most parts of Europe, especially in a broad strip extending from North-Western to South-Eastern Europe (Schär *et al.*, 2004). Seven years later the record-breaking summer of 2010 (e.g., Dole *et al.*, 2011; Rahmstorf and Coumou, 2011; Otto *et al.*, 2012; Trenberth and Fasullo, 2012; Hauser *et al.*, 2016) even exceeded amplitude and spatial extent of 2003 (Barriopedro *et al.*, 2011; Russo *et al.*, 2015), with most strongly affected areas located in Western Russia and Eastern Europe. The summers of 2003 and 2010 are the most prominent examples of recent heat extremes, because of their extreme heat intensity, duration of heat waves and large-scale spatial relevance. Furthermore, they received wide-spread attention for their elevated levels of human morbidity and mortality (Åström *et al.*, 2011; Li *et al.*, 2015) with 10.000 s of excess deaths (Robine *et al.*, 2007; Barriopedro *et al.*, 2011), largely connected to their very long and uninterrupted heat waves.

Yet, other recent summers were similarly extreme at smaller spatial or temporal scales, like July 2006 in large parts of Europe (Rebetez *et al.*, 2009; Kysely, 2010; Lhotka and Kysely, 2015a), the summers of 2007 (Busuioc *et al.*, 2007; Founda and Giannakopoulos, 2009; Unkašević and Tošić, 2011; Corobov *et al.*, 2013) and 2012 in South-

Eastern Europe, heat extremes in summers 2012 (Holtanová *et al.*, 2015) and 2013 (Lhotka and Kysely, 2015b) in Central Europe, the very intense summer of 2015 especially in Central-Eastern Europe (Duchez *et al.*, 2016; Hoy *et al.*, 2017; Krzyżewska and Dyer, 2018) and the very hot summer of 2017 in Southern Europe (Sánchez-Benítez *et al.*, 2018; Kew *et al.*, 2019). Latest examples are the exceptionally intensive heat waves of late June and late July 2019, resulting in new national heat records for France (MeteoFrance, 2019), Belgium (KMI, 2019), The Netherlands (KNMI, 2019) and Germany (DWD, 2019a), smashing the old – partly decade-old – record values by extremely large margins of a few K each.

Global warming is indeed the key factor of the high frequency of heat episodes occurring in the last decades all over the world (IPCC, 2013; Russo *et al.*, 2014; Christidis *et al.*, 2015), and further increasing heat conditions are expected by climate modellers within the 21st century (e.g., Barriopedro *et al.*, 2011; Russo *et al.*, 2014, 2015; Christidis *et al.*, 2015; Lhotka *et al.*, 2018). However, also large scale (atmospheric and oceanic) circulation variations strongly influence extreme summer temperatures in Europe (e.g., Sutton and Hodson, 2005; Jones and Lister, 2009; van den Besselaar *et al.*, 2010). Previously European summers were comparably warm from the 1930s to the 1950s, culminating in the very hot summers of 1946 (predominantly in South-East Europe) and 1947 (particularly in Western Europe, but also other areas; Hoy *et al.*, 2017). That period was connected to a higher level of continentality, especially pronounced in the 1940s (Kozuchowski *et al.*, 1994; Thompson, 1995). In contrast, warm summers were rather rare in the early 20th century and from the 1960s to the 1980s, connected to predominantly maritime air masses over Europe (Kysely, 2002). Since the 1990s, much higher temperatures (alongside an increased level of continentality) were observed during summer, and during the early 21st century, temperatures settled around the level of the extreme 1947 summer in large parts of Europe (Hoy *et al.*, 2017).

This study analyses duration, timing, intensity and spatial extent of the 2018 heat conditions in Europe in a secular time-perspective, and the possible contribution of atmospheric circulation and Atlantic Ocean temperatures.

It is based on a spatially well-distributed dataset comprising many of the longest and most reliable station time series with daily average and extreme temperature records available in Europe, with a special focus on data homogeneity. We involve a range of temperature indices and two heat wave definitions. We consider the length of individual station series to analyse the summer 2018 heat episodes into a more than two century time perspective, while we present time series for a European average for the period 1855–2018, completed by evaluations for five European regions from 1881 onwards. To explain observed variations in European summer heat, we

employ the following datasets: (a) the original (manual) and one automated version of the well-known Grosswetterlagen classification (Hoy *et al.*, 2013a, 2013b, 2013c), (b) a selection of teleconnection indices relevant for Europe (CPC, 2012) and (c) an index describing variations of the Atlantic sea surface temperatures, the Atlantic Multidecadal Oscillation (Sutton and Hodson, 2005; Sutton and Dong, 2012).

Our study is compiled the following: Section 2 introduces study area and data base and discusses data quality and homogeneity issues. It further presents temperature indices, classifications of atmospheric and oceanic circulation and methods. Section 3 gives an overview about the thermal conditions of the 2018 summer, relates them to centennial developments, and investigates the role of atmospheric and oceanic circulation. The paper finishes with a discussion of the results complemented by further seasonal and anthropogenic supporting factors of hot summers (Section 4), followed by the conclusions in Section 5.

2 | DATA AND METHODS

2.1 | Study area and data base

2.1.1 | Study area

The study area is the European continent apart of Russia east of its western borders, the eastern parts of the Ukraine and Iceland (Figure 1a). To account for regional specifics, five European regions are defined in this paper. In their compilation, we focussed on both achieving geographic consistency and a grouping of areas with similar climatic

features (Figure 1b), using continentality (winter-summer temperature difference) and average summer temperatures (Supporting Information Data S1). We also looked at the distribution of subtypes of the Köppen-Geiger climate classification (according to Beck *et al.*, 2018). All regions comprise 14 climate stations, apart of region South-East with 11 stations. The regions may be characterized the following:

- NE (North-East): cool, rather continental climate (large differences between winter and summer temperature, summer temperature around 15°C; mainly Dfc and Dfb).
- W (West): rather cool, maritime climate (small differences between winter and summer temperature, summer temperature [often considerably] below 20°C; mainly Cfb).
- C (Central): temperate summers in transition zone between maritime and continental climate (summer temperature below 20°C; mainly Dfb).
- S (South): subtropical summers (summer temperature considerably above 20°C, mainly Csa).
- SE (South-East): warm, continental climate (large differences between winter and summer temperature, summer temperature around 20°C; mainly Dfb).

2.1.2 | Data characteristics and availability

67 locations in 26 countries are included in our analysis, comprising among the longest, most complete and most

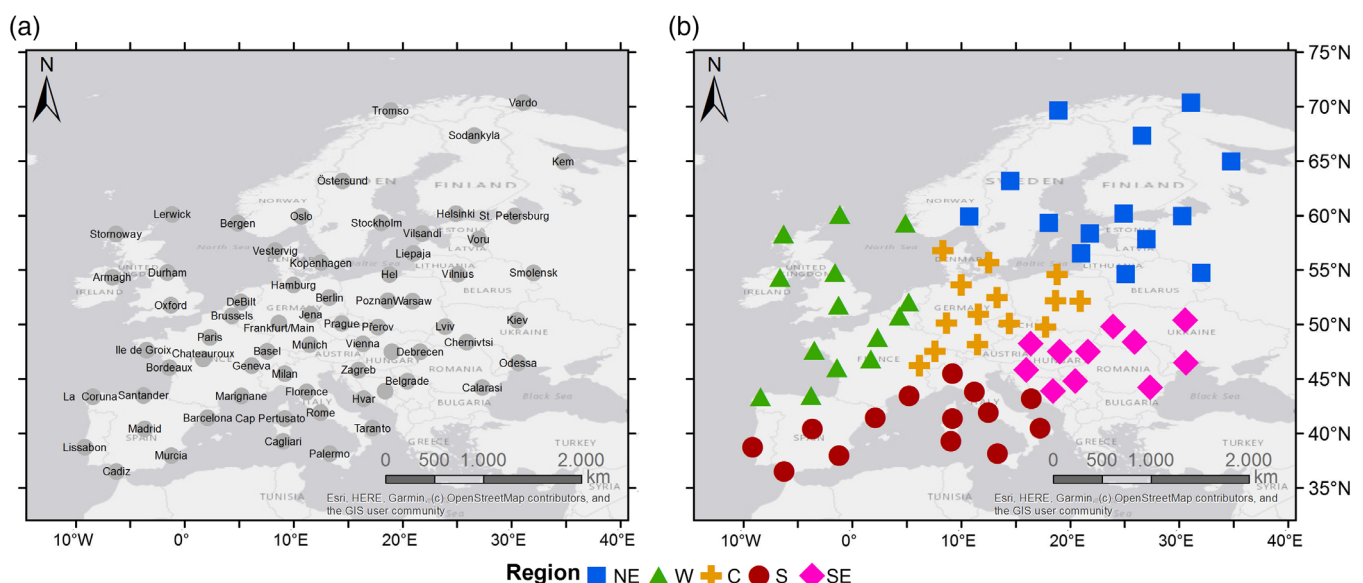
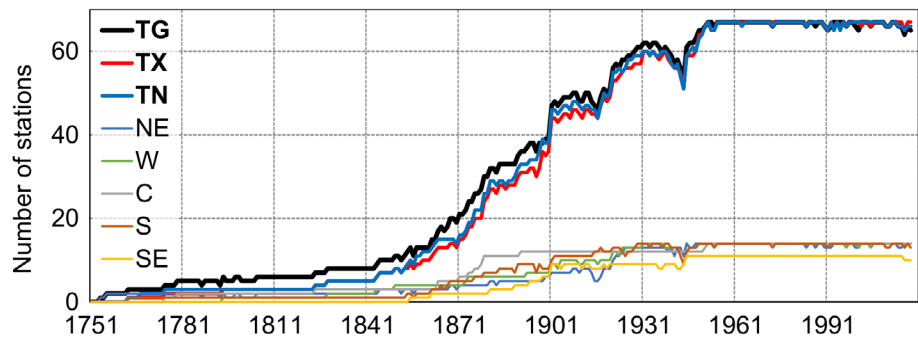


FIGURE 1 Study area with (a) name and location of the 67 meteorological stations (left) and (b) allocation into five regions (right)

FIGURE 2 Increase of data availability over time within the study area (for TG, TX and TN) and the five regions (only TG)



reliable (homogenous) daily mean (TG), maximum (TX) and minimum temperature (TN) European station time series, while at the same time ensuring an as optimal as possible spatial distribution of stations within Europe. Station density is spatially similar within the regions except for region North-East, which has more stations in its southern part ($\leq 60^\circ\text{N}$) than further north.

Table 1 presents an overview of the included stations and their data characteristics including the start year of the records. Almost all stations are located at altitudes – mostly considerably – below 500 m (three exceptions up to 667 m), with an average elevation of 124 m. Average data availability is 98.2% for all three parameters, with only two stations dropping below 90% availability. Region Central comprises the longest data series, while time series in regions North-East and South-East are, on average, shorter (Figure 2). Six stations with daily TG and three with TN/TX data (Brussels, Prague and Milan) start within the 18th century and five more stations before 1850. A clear increase of data availability gets apparent from about 1881 and again 1901, as well as a temporary drop in availability towards the end of both world wars (more pronounced for WWII). Data of all stations, with very few exceptions during single years, are available from 1951. All time series are updated until October 2018 or longer.

2.1.3 | Data quality and homogeneity

A high level of data homogeneity is crucial, because inhomogeneities may seriously affect results generated from the analysis of time series of meteorological data (Wijngaard *et al.*, 2003; Böhm *et al.*, 2010; Lundstad and Tveito, 2016). Supporting Information Data S2 illuminates potential inhomogeneity sources within time series of meteorological data and resulting problems for data analysis.

As we are investigating secular time frames, the quality of the (complete) underlying dataset determines the robustness of our study. Hence, the stations employed in this study were selected according to quality criteria – about 90% of all station time series used in this paper

underwent some form of homogeneity treatment (Table 1). We ranked data according to three different quality classes. Carefully documented homogenizations of full time series using local metadata form the best and most reliable Category 1, connected to a very high research effort per station. Only Stockholm (SE), Armagh, Oxford (both GB), De Bilt (NL), Basel, Geneva (both CH) and additionally for TG Tromsø, Bergen and Oslo (all NO) fall in that category – the relevant papers describing the performed quality controls and homogenization efforts are given in Table 1. On the other hand, only a few stations had to be allocated to the lowest Category 3, because their quality could not specifically be verified. They do not necessarily include (large) inhomogeneities, but their quality is not traceably enough for us to proof the opposite.

About 80% of our data fall in Category 2, which consists of technically homogenized data or quality-controlled original data with proven none or very little location changes. Most of the data in that category derives from a homogenized version of the original European Climate Assessment and Dataset (ECA&D) station data collective (see <https://eca.knmi.nl/dailydata/predefinedseries.php>), which itself can be considered to be the largest and most reliable source of long-term station data in Europe (Simolo *et al.*, 2014; Cioffi *et al.*, 2015; Hoy *et al.*, 2017; Squintu *et al.*, 2019). The station data relevant for this study were directly received by and discussed with A. Squintu (ECA&D). The homogenization of the ECA&D dataset was done using a quantile matching approach (Squintu *et al.*, 2019). Such an automated procedure cannot match the quality of metadata-supported performances for individual stations as in Category 1. It is yet useful for large datasets with generally missing individual metadata (Squintu *et al.*, 2019), which often would otherwise be biased by various unaccounted inhomogeneities. Be aware that ECA&D data are often blended (= added via synoptical messages) for recent months or years. Blended data have been included in the homogenization.

We checked all 67 station time series for cases of $\text{TN} \geq \text{TX}$. That procedure helped us to find cases with

TABLE 2 Description of temperature indices

| Abbreviation | Variable | Definition | Unit |
|-------------------|----------|--|------|
| SU _{av} | TG | Average summer temperatures (June to August) | °C |
| SHY _{av} | TG | Average summer half year temperatures (April to September) | °C |
| HW ₉₀ | TX | Most intense annual heat wave; onset: ≥ 3 days with periodic TX average ≥ 90 th percentile (P90) of 1961–1990 daily summer TX; single day of $< P75$ or periodic average $< P90$ ends episode; intensity: sum of daily excess temperatures $> P90$ | K |
| HW ₉₅ | TX | Most intense annual heat wave; onset: ≥ 3 days with periodic TX average ≥ 95 th percentile (P95) of 1961–1990 daily summer TX; single day of $< P90$ or periodic average $< P95$ ends episode; intensity: sum of daily excess temperatures $> P95$ | K |
| WD | TX | Warm days: days with TX $\geq 20^\circ\text{C}$ | days |
| SU | TX | Summer days: days with TX $\geq 25^\circ\text{C}$ | days |
| HD | TX | Hot days: days with TX $\geq 30^\circ\text{C}$ | days |
| TX ₉₀ | TX | Annual sum of daily excess temperatures $> P90$ of 1961–1990 daily summer TX | K |
| TX ₉₉ | TX | As TX ₉₀ but for $> P99$ | K |
| TNi | TN | Tropical nights: days with TN $\geq 20^\circ\text{C}$ | days |
| TN ₉₀ | TN | As TX ₉₀ but for TN | K |
| TN ₉₉ | TN | As TX ₉₉ but for TN | K |

wrong 0.0°C values, partly mixed TN and TX series and other problems. Many of the cases could be solved by consultation with data providers or A. Squintu in case of the homogenized ECA&D dataset, yet a few remain for 27 stations. They should not affect any evaluation of this paper, because only a few cases per station normally occur and for all but one station such cases form (much) less than 0.1% of all data (exception of Palermo with 302 cases = 0.5%; Supporting Information Data S1). Another helpful quality check was a visual inspection of the annual cycle of daily maximum and minimum values, which additionally helped to find outliers and wrong zero cases, which could be corrected in consultation with the data providers or were deleted. Additional homogeneity information for individual stations can be found in the last column of Supporting Information Data S1.

2.2 | Temperature indices

The variability of (summer) heat conditions is explored via temperature indices described in Table 2. They

mainly derive from publications of the World Meteorological Organisation (WMO; Klein Tank *et al.*, 2009) and the ECA&D project (ECA&D, 2013). Percentile-based thresholds support a regionally comparable evaluation of seasonal characteristics, independent of climatic characteristics based on the geographical location or local specifics. Fixed thresholds impede comparisons in regions characterized by diverse climatic conditions (Shevchenko *et al.*, 2014; Lhotka and Kyselý, 2015a), yet help understanding regional climatic peculiarities (Kyselý, 2002, 2010). Therewith, the gradual change from cool and/or maritime conditions in Western and Northern Europe to the warm and/or continental climate of Southern and Eastern Europe gets visible.

We use percentile-based indices as summation of all temperatures over the particular thresholds, while the days of occurrence are used for fixed thresholds. Heat wave characteristics are explored using percentiles of the local summer temperature distribution. Compared to other approaches (see summary in Lhotka and Kyselý, 2015a), typically using a three-day-onset with temperatures over a certain threshold, we decided for a slightly ‘softer’ onset, as we accepted a 3-day-average over

the particular threshold. We use two heat wave definitions to account for longer intense (HW_{90}) and shorter very intense (HW_{95}) cases. A heat wave continues as long as the average over all previous days of the same heat wave stays above the threshold, and as long as the abort criteria of a single day below the 75th (HW_{90}) or 90th percentile (HW_{95}) is not met (Table 2).

2.3 | Classifications of atmospheric and oceanic circulation

Indices and classifications condense the manifold variations of atmospheric circulation conditions into straightforward schemes of index values and circulation classes, determined by similar atmospheric processes like comparable (a) geographical distributions and spatial movements of driving pressure areas (anticyclones, cyclones, troughs and ridges), (b) air mass inflow directions and (c) air mass attributes.

We use two versions of the well-known Grosswetterlagen classification: (a) the original manual Grosswetterlagen classification (GWLc; Baur, 1947; Hess and Brezowsky, 1977) and (b) an automated version, the SynopVis Grosswetterlagen classification (SVGc, version 2019) developed by Paul James (personal communication; see also Hoy *et al.*, 2013b). The classification scheme is chosen for its proven large-scale relevance within Europe (James, 2007; Huth, 2010). For an enlarged overview about (a) the historical development of the classification, (b) the composition, character and trends of circulation types, (c) the spatial response to sea level pressure and (d) temperature in Europe and adjacent areas see Hoy *et al.* (2013a, 2013b, 2013c). We use 10 major circulation types, based on air mass inflow into Central Europe and cyclonicity in this area (James, 2007; Werner and Gerstengarbe, 2010). Therewith, we characterize the 2018 SHY. We employ GWLc data derived from Werner and Gerstengarbe (2010), updated until 2018 by monthly publications of the German Weather Service (DWD, 2019b). SVGc data were provided by Paul James.

The North Atlantic Oscillation is the most prominent teleconnection impacting the study area. It describes the intensity of westerlies as related to the pressure difference between Icelandic Low and Azores High (Hurrell, 1995). The North Atlantic Oscillation index (NAOI) used here derives from Li and Wang (2003), updated via <http://ljp.gcess.cn/dct/page/65610>. This NAOI shall provide a more faithful representation of the spatial-temporal variability associated with the NAO in all seasons compared to other (all-year) NAOIs, which are often relevant for the north-hemispheric winter half year only (Li and Wang, 2003).

Five other teleconnection indices derive from the CPC webpage (<http://www.cpc.ncep.noaa.gov/data/>

teledoc/telecontents.shtml; see details there) and have been used in a number of recent publications (e.g., Bueh and Nakamura, 2007; Moore and Renfrew, 2012; Rust *et al.*, 2015). These are:

- 1 East Atlantic Pattern (EA)
- 2 East Atlantic – Western Russia Pattern (EAWR)
- 3 West Pacific Pattern (WP)
- 4 Scandinavian Pattern (SCAND)
- 5 Polar/Eurasia Pattern (POLEUR)

The EA is structurally similar to the NAO, but its two pressure centres are shifted south-eastwards compared to the typical NAO dipole. EAWR consists of four main circulation anomaly centres, located (a) over Europe and Northern China and (b) of opposite sign over the Central North Atlantic and north of the Caspian Sea. WP is the primary mode of low-frequency variability over the North Pacific, but affects European climate as well. SCAND inheres a primary circulation centre over Scandinavia and weaker centres of opposite sign over Western Europe/Eastern Russia. The POLEUR is characterized by negative geopotential height anomalies over the polar region and positive ones over Northern China/Mongolia. The positive (negative) phases reflect a stronger (weaker) circumpolar vortex.

The Atlantic Multidecadal Oscillation (AMO) is defined as a long-term cycle in North Atlantic sea surface temperatures (SST) with positive (warmer) and negative (cooler) phases of approximately 30–40 years duration, presumably driven by the Atlantic Thermohaline Circulation decadal-scale oscillation (Knight *et al.*, 2005). Such changes have been occurring for at least the past 1,000 years and are natural. Data used here derive from the Earth System Research Laboratory of the US National Oceanic and Atmospheric Administration (<http://www.esrl.noaa.gov/psd/data/timeseries/AMO/>) and are available from 1856. The time series are calculated from the Kaplan SST data set in $5^\circ \times 5^\circ$ resolution (Kaplan *et al.*, 1998, updated monthly). The weighted area average SST are calculated over the North Atlantic ($0\text{--}70^\circ\text{N}$) and time series are de-trended (Enfield *et al.*, 2001).

2.4 | Methods

Peculiarities of 2018 and a comparison to earlier temperature variability is illustrated via a) maps of the record years since start of the individual time series given in Table 1 and b) time series calculated from the averages of all five regions for the period 1855/1881–2018. This approach of using twofold study periods for the station and the regional data enables us to assess the extremity

of the 2018 summer at individual stations for the longest available instrumental datasets, while additionally allowing for a regional estimation of its extremeness with a comparatively dense and high-quality data set for a common 164/138 year period. Data from 1855–1880 are shown in light colours to account for their lower station data coverage. From 1855, all regions comprise at least one location with TG, TN and TX data, while from 1881 all regions are covered by at least three stations. The time series of the study area average are supplemented by the top/bottom 5 years of the five European regions for the period 1881–2018 (symbols in the same illustrations) to account for regional peculiarities.

The presented teleconnection indices have been correlated (Pearson correlation coefficient) with time series of our temperature indices for the entire study area and the five regions for the period of data availability 1951–2018 for summer and additionally the previous spring and winter. Such correlation values may be affected by similar – causal or non-causal – trend behaviour. In order to focus our correlation analyses on year-to-year variability only, linear trends have been removed before calculating the correlation coefficients (detrending). Note that other kinds of trends, as well as coherent variations on decadal scales, may still be present.

3 | THE LONG, HOT EUROPEAN SUMMER OF 2018

3.1 | The summer of 2018 – An overview

Persistent and often large positive anomalies from reference climatology (1961–1990) characterized the year 2018 in Europe, which (typically) were more pronounced for maximum than minimum temperatures (Figure 3). After a cold March, April and May were (by far) the warmest

since start of observations in our station collective, both setting new monthly records at about 30% of all included stations (not shown). During April, positive anomalies were extraordinary high in region South-East with a monthly anomaly of +5.2 K (previously largest anomaly was 2000 with +3.4 K, not shown), but also record-high in large areas of Central and Southern Europe. During May, positive anomalies were more evenly distributed, covering most of Europe apart of the Mediterranean. The extraordinary warm start into the extended summer season resulted in a considerable number of days over certain thresholds, like summer days (SU), already early in summer. Temperature anomalies were less severe in June, but strongly elevated again in July. Here, the longest and most intense heat wave of this summer started in region North-East (Section 3.2), later also severely affecting Central and Western Europe. At the end of July, new all-time records of maximum and highest minimum temperatures were recorded especially in Scandinavia (Supporting Information Data S3). A different short, but extremely intense heat wave struck the Mediterranean (mainly its western parts) at the beginning of August (Section 3.2). September was very warm in wide-spread areas apart of its final days, with a high number of SU especially in Central Europe. Lastly, mid-October provided a furious final of the 2018 summer, with high maximum temperatures and wide-spread SU in large areas of Europe.

Not surprisingly, positive temperature anomalies of the 2018 SHY (April–September) were more pronounced than those of the summer season (June–August), with 2018 by far the warmest SHY in Europe (2.7 K compared to 1.9 K in 2003; Figure 4a), but ‘only’ second-warmest summer (2.5 K compared to 2.6 K in 2003; Supporting Information Data S4). 2018 was the warmest SHY in four regions and second-warmest in region South. Anomalies were largest in Central Europe, with an average regional anomaly of +3.4 K, with higher local values (+4.0 K in

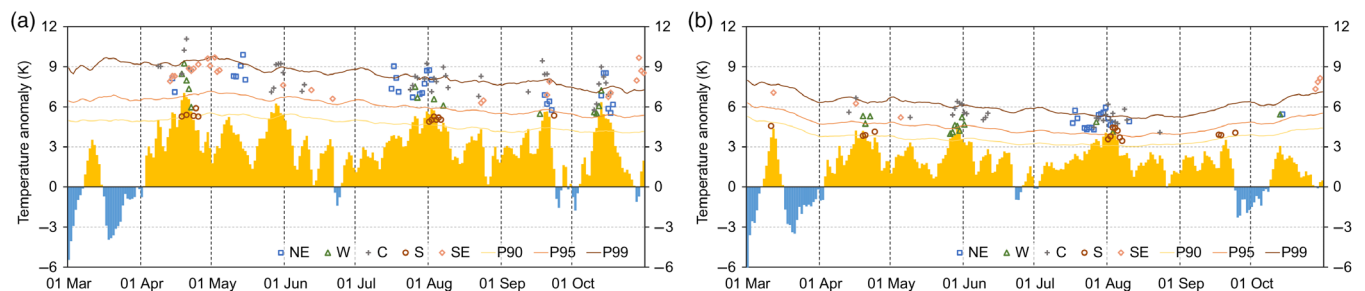


FIGURE 3 Daily 2018 mean (a) TX (left) and (b) TN (right) temperature anomalies from the shifting 11-day-centred 1961–1990 mean maximum/minimum temperatures for March to October. The 90th, 95th and 99th percentiles of the 1961–1990 temperature range are indicated by shifting 11-day-centred means. Days with ≥ 95 th percentile in 2018 are marked for the area mean of the five regions

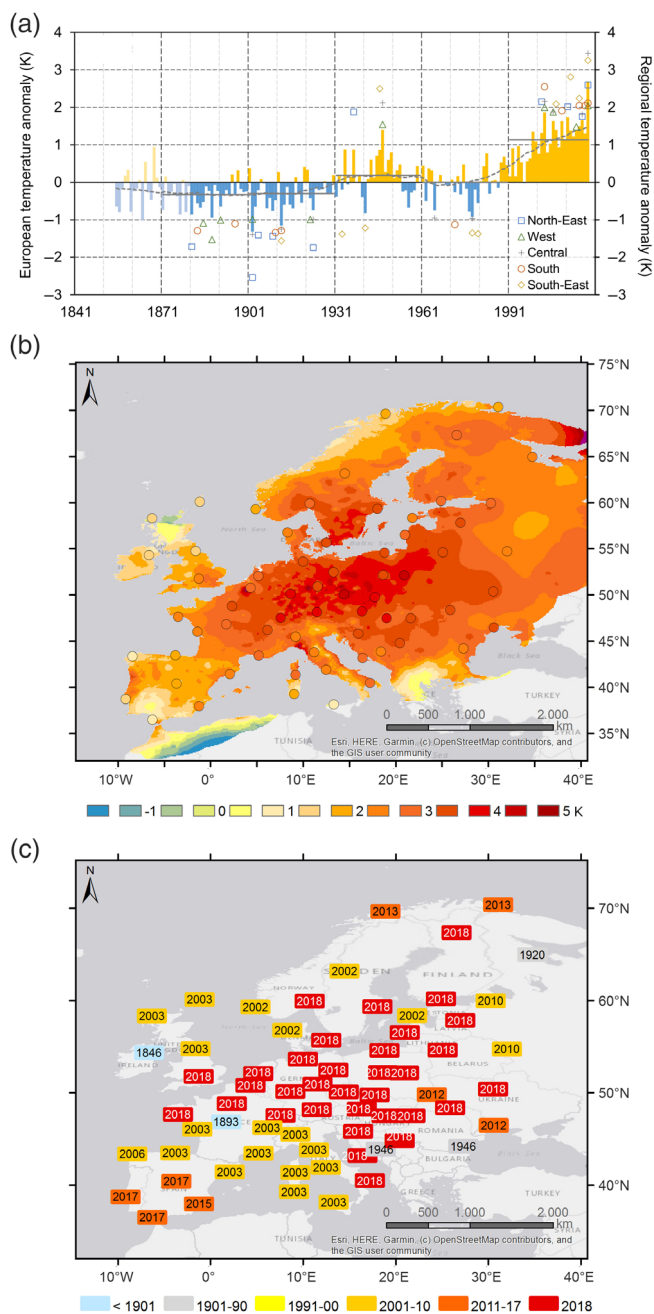


FIGURE 4 (a) Time series plot of mean SHY temperature anomalies (SHY_{av} , with respect to 1961–1990) averaged over the study area for period 1855–2018 with fixed 30-year (grey continuous lines) and moving 31-year (grey dotted lines) averages, the five most extreme positive and negative anomalies of the five regions are indicated by symbols (upper picture), (b) 2018 SHY_{av} anomaly map (in K) comparing E-OBS gridded data with the 67 meteorological stations used in this study (middle picture), (c) map of record years of highest SHY_{av} (lower picture; analogue figures for SU_{av} in Supporting Information Data S4)

Warsaw and Prague, both Central). During summer, 2018 was scarcely warmer than 2003 in the Central region and second in North-Eastern and Western Europe.

Largest anomalies were observed in Prerov and Frankfurt (+3.8 K, both Central). Figure 4b shows the SHY temperature anomalies of the gridded E-OBS data and our 67 climate stations, with a very good agreement among both datasets. The areas with the strongest positive anomalies extend from central France, Switzerland and Northern Italy towards Southern Fennoscandia, the South-Eastern Baltic Sea area, Belarus and the North-Western Ukraine. Weakest signals appear near the Atlantic coast line around the British Isles and the Iberian Peninsula. Spatial patterns for summer show a similar spatial picture (Supporting Information Data S4).

Figure 4c illustrates the record years of the locally warmest SHY since start of observations for our 67 stations. 2018 finished warmest at half (33) of all stations – within a large area from the Baltic Sea region over Europe's central latitudes towards South-Eastern Europe. The year 2003 stays warmest at 14 stations, while other years were warmest at 1–4 stations only. The 2018 summer season was warmest in a smaller region, extending from Southern England via the Southern Baltic Sea region into Poland (10 stations; Supporting Information Data S4). During summer, the year 2003 still strongly dominates the picture with records from the UK towards Central and Southern Europe (24 stations), while other summers again only cover 1–4 stations.

3.2 | Temperature indices in 2018 and in a long-term perspective

The number of days with maximum temperatures over the fixed thresholds 20°C (WD) and 25°C (SU) was extreme in 2018 in large areas of Europe, with about half of all our stations (WD: 37; SU: 33) exceeding their previous records (Figure 5c,d) – often by large margins (Supporting Information Data S3). The wide-spread appearance of new record values results from the intense heat in North-Eastern Europe (where such days are typically rare) combined with the long duration of warm conditions from April until October in other regions. New record values were observed at almost all stations in regions Central and South-East, many in regions North-East and West, and some in region South. 24 (WD) respective 15 stations (SU) exceeded their previously highest values by more than 10 days – with largest exceedances for WD reaching 28 days in Warsaw (2018:132 days, since 1951) and 26 in Berlin (160 days, since 1876, both Central), and for SU 23 days in Jena (102 days, since 1824, Central) and 18 at three other locations in regions Central and South-East. Consequently, 2018 had a much larger frequency anomaly of WD and SU in 2018 than previously observed (Figure 6c,d). All regions (apart of region South for WD)

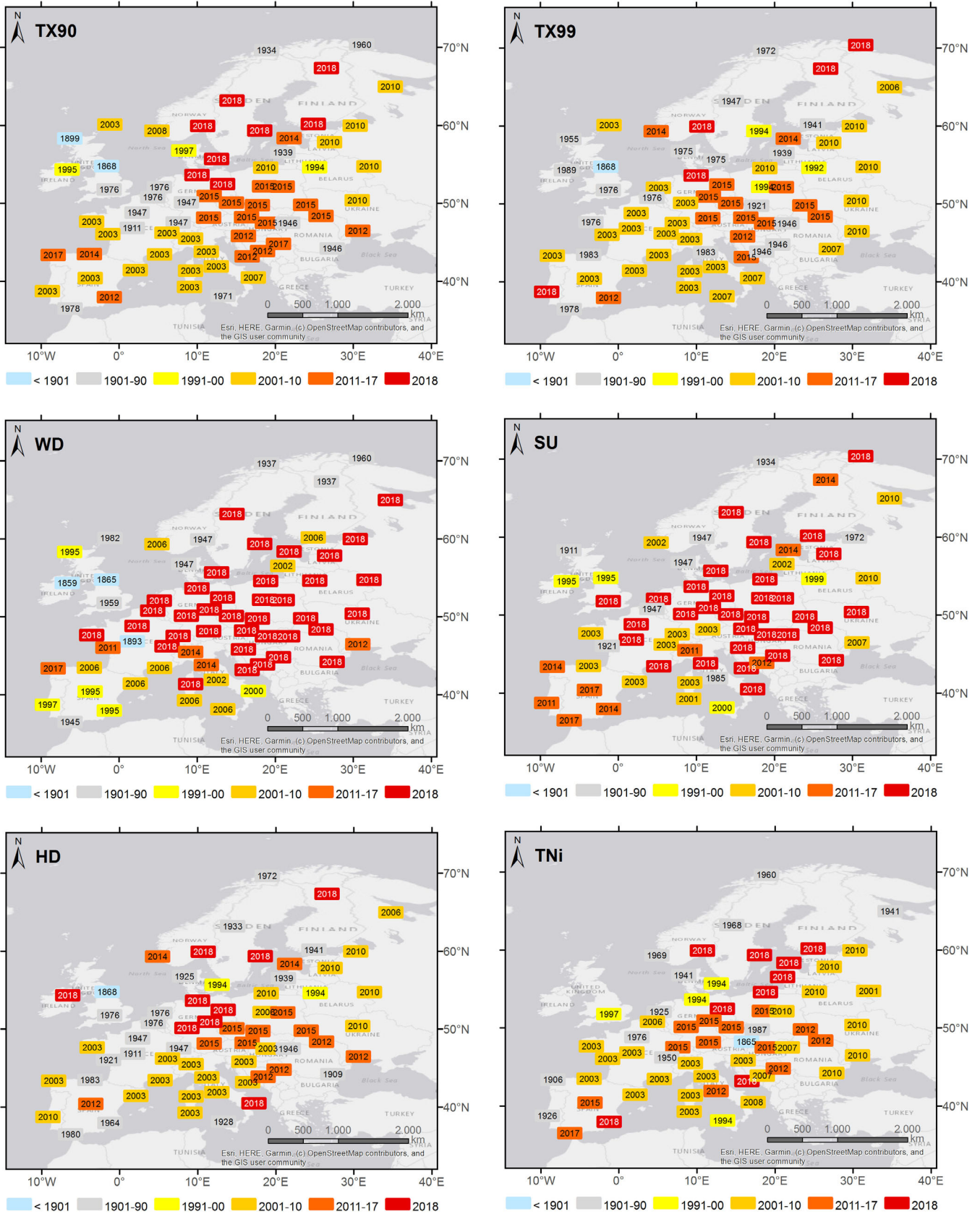


FIGURE 5 Maps of 10 temperature indices showing record years of all stations (percentile-based indices: Maximum value of temperature sum; threshold-based indices: Maximum occurrence of days); 2018 dark red with white font colour

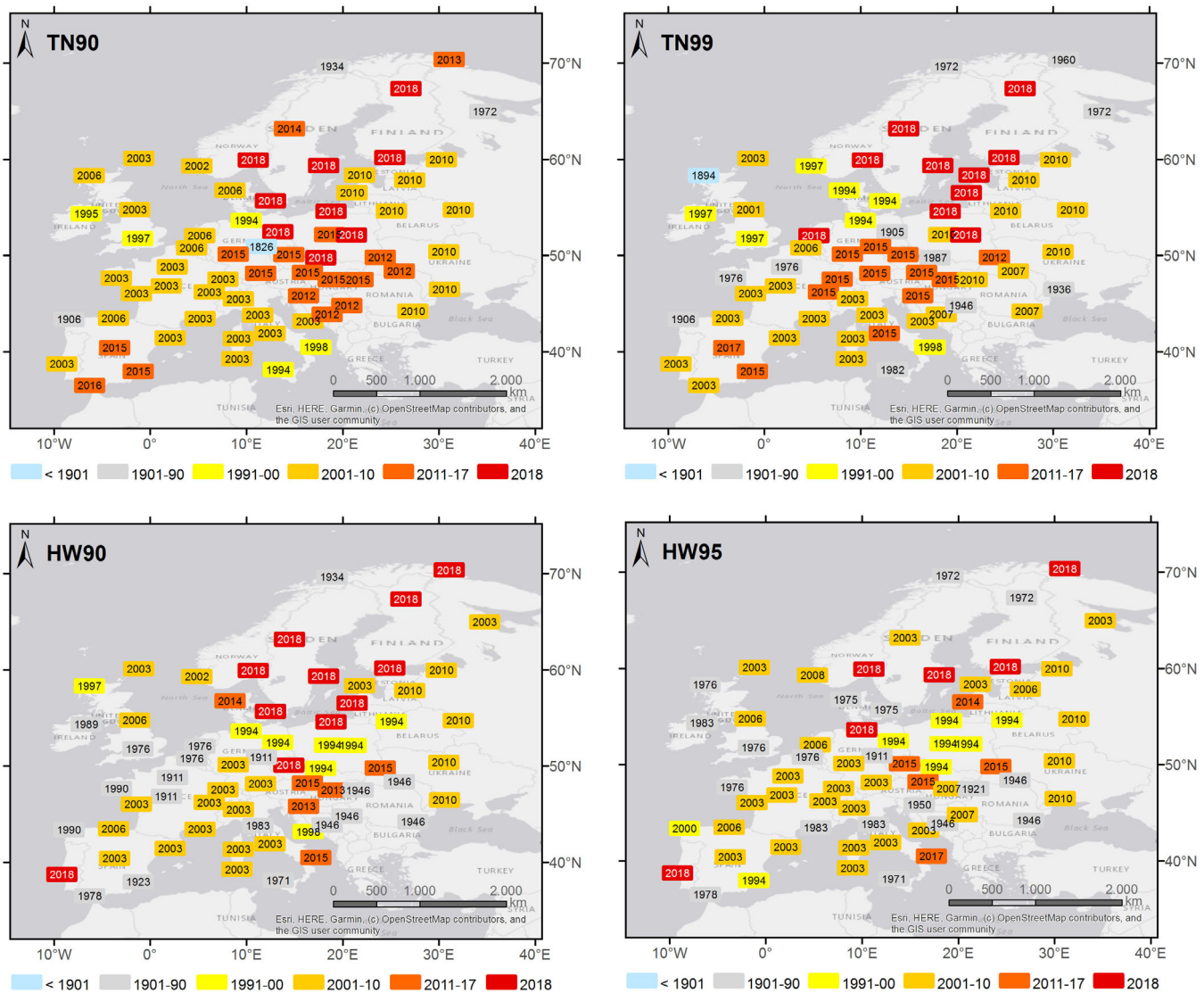


FIGURE 5 (Continued)

experienced new regional maxima in 2018, which were most pronounced in region Central, followed by regions South-East, North-East and West.

Hot days with maximum temperatures above 30°C (HD) did not break as many records as the previously discussed two indices, connected to less intense heat than other record years in southern and central latitudes and because of their general rarity in Northern Europe. They reached new maxima at 10 stations in Scandinavia and Germany, with 8 days over the previous record in Stockholm (18 days, since 1859, North-East) and 7 in Berlin (28 days, since 1876, Central). 2018 scores third among the years with maximum number of hot days, being second in region Central, third in region North-East and fourth in region South.

Temperature sums of maximum temperatures over certain percentile-based thresholds (TX_{90} and TX_{99})

reached new maxima at a number of stations in Scandinavia and Germany (Figure 5a,b). The new record values were regionally extreme, like for TX_{90} in Stockholm (136 instead of 88 K, since 1859, North-East), Copenhagen (106 instead of 68 K, since 1874, Central) and Oslo (159 instead of 113 K, since 1937, North-East; Supporting Information Data S3). Within Europe, 2018 scored third for TX_{90} and sixth for TX_{99} , but largest for TX_{90} in region North-East and Central, and second-largest in region North-East for TX_{99} , (Figure 6a,b). In a long-term perspective, 3 of 4 (TX_{90}) and 2 of 3 (TX_{99}) of all extremes were recorded after the year 2000 (Figure 5a,b).

The three indices of high minimum temperatures used here (TN_i , TN_{90} and TN_{99}) reached new maxima at about 10 stations in 2018, mainly distributed around the Baltic Sea (Figure 5f-h). Most striking were the very warm nights in Stockholm (since 1859, where the record

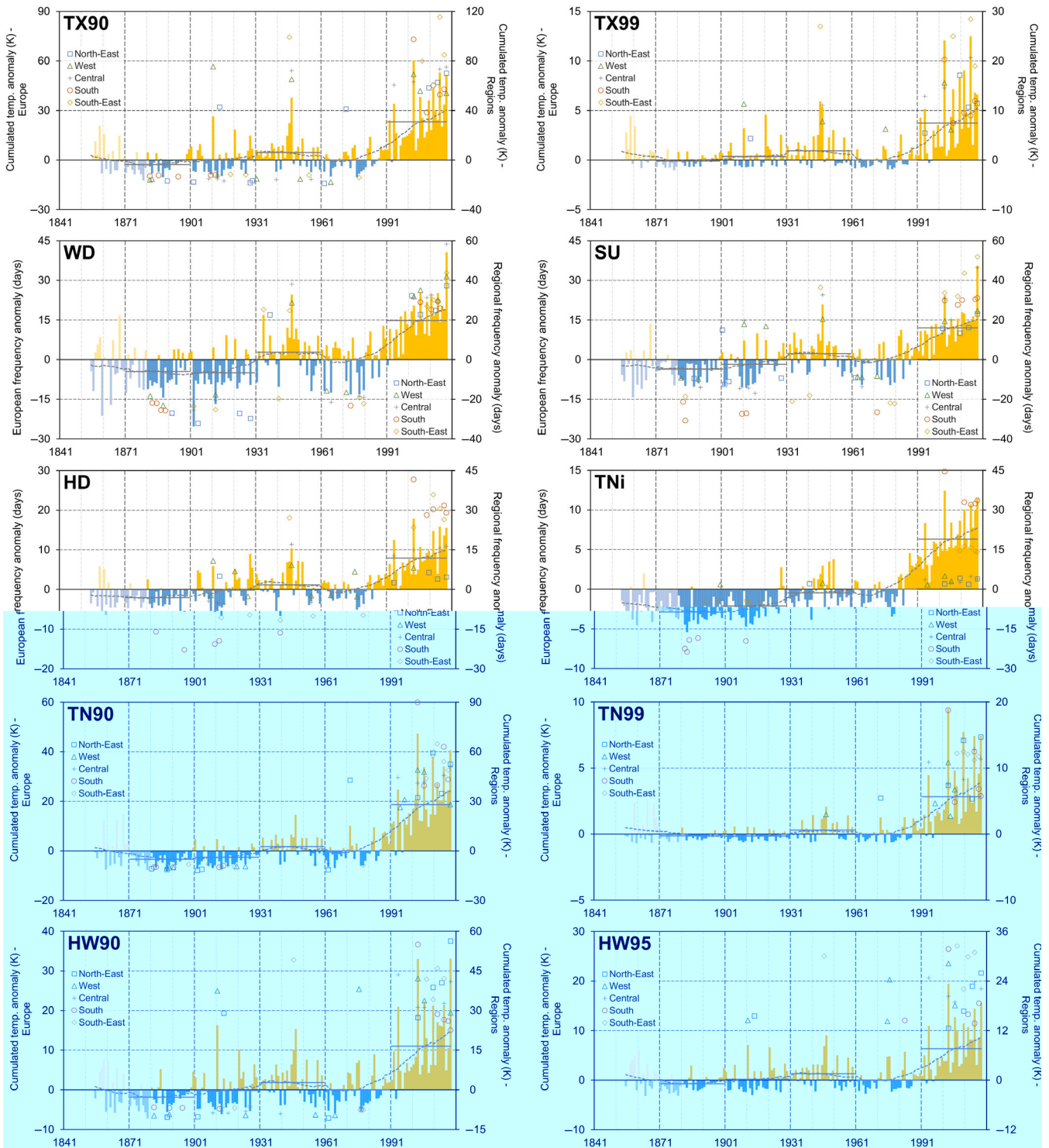


FIGURE 6 Time series plots of 10 temperature indices comprising anomalies (with respect to 1961–1990) averaged over the study area for the period 1855–2018 with fixed 30-year (grey continuous lines) and moving 31-year (grey dotted lines) averages, the five most extreme positive and negative anomalies of the five regions are indicated by symbols

number of TNi increased by 7 to 12 days and the summation of high minimum temperatures increased from 76 to 111 K (TN₉₀) and 18 to 38 K (TN₉₉), respectively. Generally, 2003 is still very present in regions South and West,

while 2015 dominates in region Central, 2010 in region North-East (mainly it is eastern areas) and 2012 in region South-East. Hence, 2003 is still, by a considerable margin, on top on the European level, with 2018 on second or

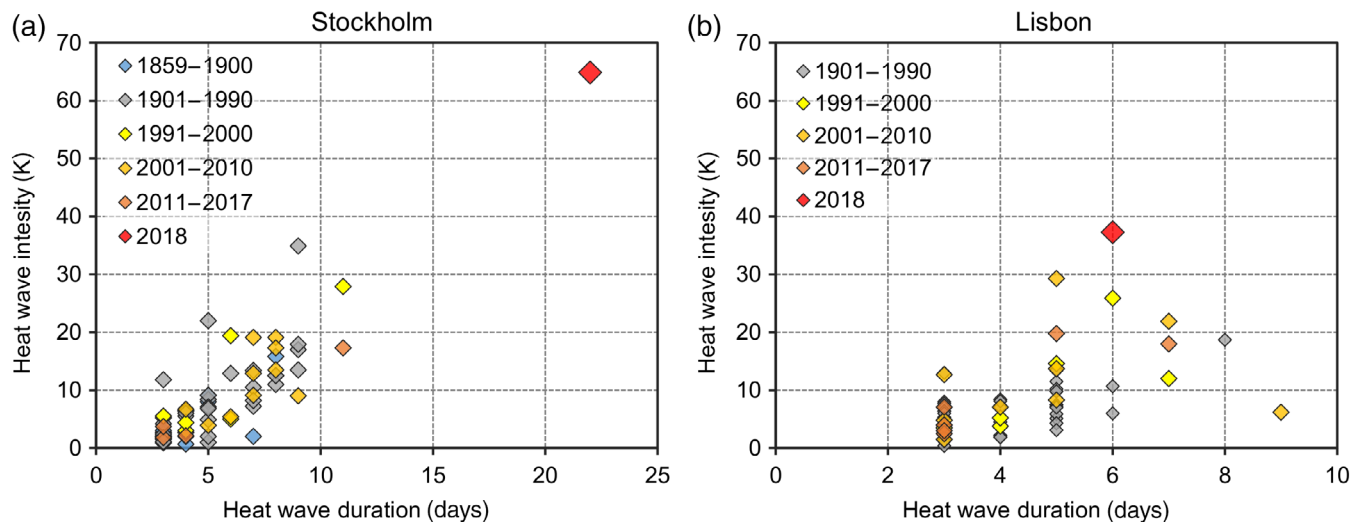


FIGURE 7 Heat wave evolution of the most intense annual HW_{95} for (a) Stockholm (left) and (b) Lisbon (right; be aware that heat waves do not occur every year)

third rank (Figure 6f–h). Regionally, 2018 claims the first rank for TN_{90} in region Central and for TN_{99} in region North-East.

Two approaches of heat wave definition (see Section 2.2) are used, one with high (over the 90th percentile; HW_{90}) and another with very high (over the 95th percentile; HW_{95}) threshold values. A very intense heat wave developed in the latter two decades of July and the first of August, spatially comprising large areas around the Baltic Sea region, where it was the most intensive heat wave since start of observations at 10 (HW_{90}) or 5 (HW_{95}) stations (Supporting Information Data S3). That heat wave manifested itself especially strongly at the very reliable and long-term observatory of Stockholm (TX data from 1859, North-East). On basis of HW_{95} it was – by far – the most intense (65 compared to 35 K in 1975) and longest (22 instead of 11 days) heat wave ever recorded there (Figure 7a). If we employ our heat wave definition to TG instead of TX values – as Stockholm comprises the longest daily TG records in Europe, starting in 1756 – the heat waves of 1819 (27 days) and 1911 (20 days) were comparably long as 2018 (24 days), but the extreme intensity of 2018 stays unprecedented (2018:71 K, 1781:39 K). Concerning heat wave intensity, also HW_{90} saw a doubling of previous Stockholm records (100 compared to 53 K in 1975), which remains true if we apply TG values again (2018:110 K, 1846:65 K).

A separate, spatially and temporally much smaller, but extremely intense heat wave developed around the Western Iberian Peninsula in the first days of August. It was the most intense heat wave ever recorded in Lisbon, despite its length of only 6 days for both HW_{90} and HW_{95} . During its peak at fourth and fifth of August it

topped all previous records of daily maximum TX, TG and TN at this station by a margin of 1 K or more (data since 1901; TX: 43.3°C compared to previous maximum of 41.8°C). Figure 7b shows the evolution of heat waves in Lisbon for HW_{95} , with a strong increase in heat wave intensity (but not length) getting visible from the 1990s.

For all stations a list of the 2018 and (previously) highest values of all employed indices (Table 2), as well as the (current) record years, is provided in Supporting Information Data S3.

3.3 | The 2018 summer and atmospheric and oceanic circulation

3.3.1 | Grosswetterlagen

The Grosswetterlagen classification was developed for Central Europe (Germany), but has a considerable larger-scale relevance within Europe (Section 2.3). Comparing the number of certain patterns of the 2018 SHY to the average over the period 1951–2018, patterns with continental inflow from eastern and southern directions (NE, E, SE, S; GWLc 40% instead of 27%; SVGc 47% instead of 33%) as well as anticyclones centred over Central Europe (GWLc: 19% instead of 16%; SVGc: 21% instead of 15%) were prevailing. During the summer months (as a combined effect), they are typically associated with mainly warm and rather dry weather, especially towards regions North-East, West and Central (Hoy *et al.*, 2013c). Considerably less situations with westerly to northerly air mass inflow into Central Europe (W, NW, N; GWLc 33% instead of 47%; SVGc 26% instead of

42%) occurred during the SHY. They typically bring rather cold and humid air masses into most parts of Europe – again with focus on previously mentioned regions (Hoy *et al.*, 2013c). Additionally, during 2018 more days than usually were classified as anticyclonic in Central Europe (GWLc: 51% instead of 47%; SVGc: 62% instead of 48%), which during the SHY typically supports warm, dry and sunny conditions.

3.3.2 | Teleconnection indices

In the east of Europe, a positive EA during summer is associated to anticyclonic conditions and southerly inflow (Rust *et al.*, 2015), supporting positive temperature anomalies there. In 2018, the EA index was third highest since 1951 (after 2017 and 2016) during both summer and SHY, with a new maximum value in July, where the strongest heat wave of this summer was observed. Correlation coefficients show that above-average EA values during spring and summer are related to warmer European summers, their relevance increasing from west (no signal) to east (strong signal; Supporting Information Data S5). Accordingly, the rather chilly summers of the 1961–1990 decade were accompanied by low EA summer values (average of -0.6), while the hot summers after the millennium occurred during high EA values (average of $+0.7$; Figure 8). In fact, the 10 warmest summers within the study region all occurred between 2002 and 2018.

Northerly air mass inflow towards Western Russia dominates the positive phase of the EAWR during summer (Rust *et al.*, 2015), consequently leading to a negative relation with warm summers/hot temperature extremes in the very east of Europe (in our study this relation is mainly visible in region South-East; Supporting Information Data S5). The positive phase of WP is characterized by low pressure over most of study area during summer (CPC, 2012), hence supporting cooler European summers. During the summer of 2018 index values of both indices were low (WP third lowest together with 2002). Accordingly, the indices of both EAWR and WP during the cool summers of 1961–1990 were high ($+0.6$), while they were pretty low after the year 2000 (-0.4 ; Figure 8).

The positive phase of SCAND relates to high pressure and warmer summer temperatures over Scandinavia (Rust *et al.*, 2015), which gets apparent in region North-East (Supporting Information Data S5). Stronger negative relations yet appear in the south, where low pressure is prevailing (regions South-East and South). The 2018 index values were unremarkable, but May and July, the months with the largest positive temperature anomalies in region North-East, displayed record high index values (in agreement with the very stable Scandinavian

anticyclone during that time; WWA, 2018). Both months were very warm in Scandinavia and region North-East, but rather unremarkable in region South and (only July) South-East.

There is no explanatory power of the used NAOI related to warm summers in Europe (Supporting Information Data S5), for region Central in agreement with Kysely (2002), who found only weak relations between a different NAOI and Prague summer mean and cumulated extreme temperatures. The only exception is a tendency towards less common high temperature extremes during the following summer in region North-East with prevailing positive winter NAOI values, possibly related to abundant precipitation and snow cover during winter in this region, which may impede early soil drying during spring and early summer. Also, relations between temperature indices and POLEUR are weak. Exception is, again, a tendency towards lower summer temperatures in region North-East with positive index values in spring and especially winter, which cannot be explained here.

3.3.3 | Atlantic multidecadal oscillation

We find a strong positive correlation of the European summer temperatures since the early 20th century with the AMO time series for our study area, which is specifically visible when smoothed over a number of years (a smoothing of 11 years results in a correlation of >0.5 ; from 1901 in >0.8 ; Figure 9a). Relations in early decades are weak, which considerably reduces the calculated correlations. The influence of time lags on the magnitude of correlations was checked on a yearly scale for various smoothing values. Results confirm the assumed multidecadal character of the AMO, with high correlation values of ≥ 0.5 (for 11-year smoothing) between the respective current summer temperatures with AMO values up to at least 10 years in the future. Correlations

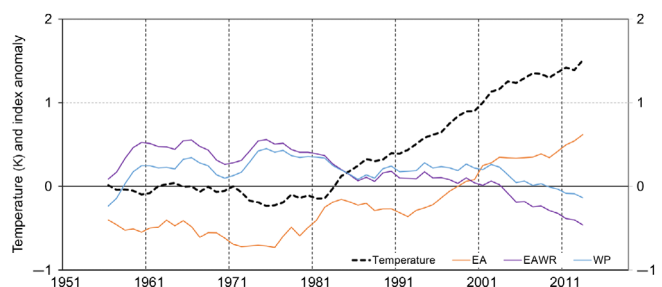


FIGURE 8 Centred 11-year summer (JJA) averages of the study area mean temperature (dashed black line) and average index values of three teleconnection indices (CPC, 2012), period 1951–2018

are similarly large for 3-, 5- and 11-year smoothing, and less visible for yearly values (Figure 9b). Differences between original and de-trended series are negligible (Supporting Information Data S6).

4 | DISCUSSION

4.1 | Temperature

The most striking characteristics of the 2018 summer were new European records of SHY_{av} , combined with strong positive deviations in the number of daily maxima over 20°C (WD) and 25°C (SU). All three indices are interlinked and point towards the long and persistent positive temperature anomalies that characterize the 2018 summer. The new records are largely due to the shoulder seasons: April and May were the warmest in our station collective since observation start, while September and October included a high number of days with summery conditions as well. Additionally, July and August were characterized by one of the most persistent and intensive heat waves since beginning of instrumental records in regions North-East and Central.

The 2018 summer brought extreme temperatures in two regions, (a) Scandinavia and nearby regions, with new highest maxima at five stations and new highest minima at six stations (Supporting Information Data S3) and (b) the Iberian Peninsula, with new all-time maxima in Madrid and Lisbon – connected to the short, but unprecedentedly intensive heat wave of only 6 days from first to sixth of August 2018. Locally, most new records occurred at the very reliable and long-term station of Stockholm (10 of 12 temperature indices, data since 1858, North-East). Five to nine new index records were obtained in Oslo, Helsinki, Sodankylä, Östersund (all

North-East), De Bilt (West), Copenhagen, Hel, Warsaw, Prague, Prerov, Hamburg, Berlin and Jena (all Central) – see summary of our results in Figure 10. Strongest signatures of the mid-summer heat wave appeared around Sweden, where all Swedish and nearby stations show strong new maxima for HW_{90} . The spatial distribution of index records confirms that the region with the most unusual temperatures was centred over the South-Western Scandinavian Peninsula, with strong positive anomalies extending in all directions around the Baltic Sea (Figure 10) – supported by distinct and long-lasting anticyclonic conditions in this area (WWA, 2018).

Examining the continental/regional perspective since availability of such data, almost all indices show two maxima directly after 1855 (not robust as possibly biased by low data availability and limited data quality, respectively; see Sections 2.1 and 2.4) and around the 1940s. Yet, the high levels since the 1990s, which are further accelerated since the hot summer of 2003, are striking and unprecedented (Figures 4a and 6; Russo *et al.*, 2015; Christidis *et al.*, 2015; Dong *et al.*, 2017; Manning *et al.*, 2019). The last year within the regional low TOP5 (cold extremes) of any index is therefore the year 1980, while a large majority of all regional high TOP5 (warm extremes) of any index is found from 1992 onwards. That signal is specifically strong for high percentiles of minimum temperatures (TN_{90} and TN_{99}), where nearly all regional TOP5 occurred after 1992.

Heat waves show similar temporal maxima like discussed before (after 1855, around 1940s, from the 1990s intensifying from 2003 onwards). The most intense HW_{90} 2018 heat waves were, at our 67 stations, similarly intense like the 2003 ones, which mainly refer to the first two decades of August 2003. Concerning HW_{95} 2003 stays clearly first, with 2018 following behind (Figure 6i,j). If all heat waves of a year are summed up within the

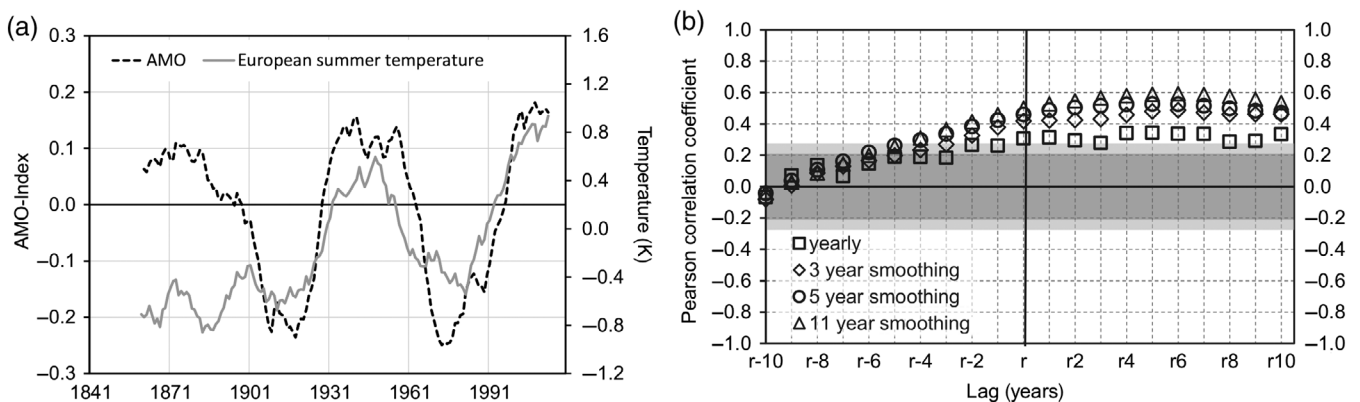


FIGURE 9 (a) Centred 11-year averages of AMO and average study area SU_{av} ; de-trended values for period 1855–2018 (left) and (b) Pearson correlation coefficients for yearly and smoothed time series of AMO and SU_{av} for lags from –10 to +10 years for period 1855–2018 (right; de-trended for 1855–2018)

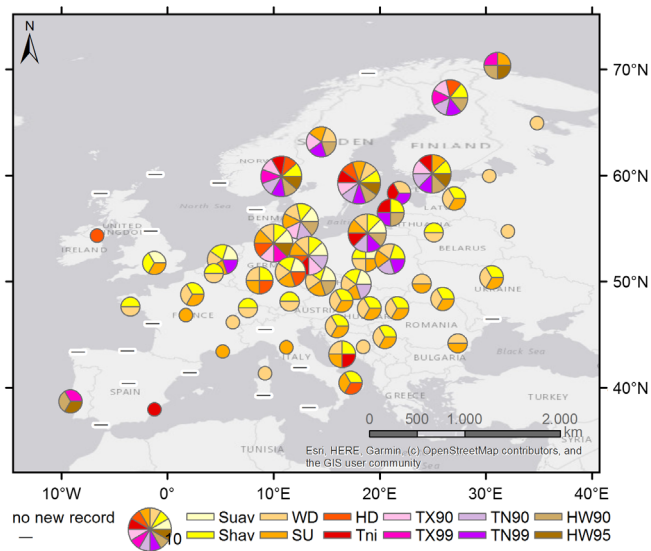


FIGURE 10 Graphical summary of number and characteristics of new record values since start of respective observations at our 67 stations

67 stations, 2018 ranks third (HW_{90}) or fourth (HW_{95}), respectively, in the European perspective (not shown). Here, the year 2015 gets strongly visible, which was characterized by a number of very intense, but mainly short heat waves (Hoy *et al.*, 2017).

4.2 | Atmospheric and oceanic circulation and hot summers

During the SHY 2018 both manual (GWLc) and automated (SVGc) Grosswetterlagen classifications often show the same (51% of all days) or related circulation patterns at a certain day, sometimes lagged by 1–2 days. The high level of similarity is remarkable, considering general difficulties to reproduce manual (subjective) classifications by automated methods, as well as methodical differences. We showed that the long and pronounced heat conditions of the 2018 SHY were supported by a combination of favourable circulation facts. Such conclusions are also confirmed by a study of Kysely (2002) for Prague, who found that anticyclonic conditions and inflow from easterly to south-westerly direction (major types E, SE, S and SW) were responsible for 75% of all heat waves there. Within (2018 mostly affected) regions North-East and Central especially the very stable anticyclone over Scandinavia (WWA, 2018; Kornhuber *et al.*, 2019) was responsible.

Earlier studies relate a significant part of summer temperature variability in Europe to the AMO (Sutton and Hodson, 2005; Sutton and Dong, 2012). Knight *et al.* (2006) show a strong relation between observed and

simulated Central England temperatures (Parker and Horton, 2005) and the AMO for summer (and autumn). Kysely (2010) found the positive/negative phase of the AMO almost perfectly corresponding to increased/decreased heat wave severity in Prague and Della-Marta *et al.* (2007) that the AMO is a possible predictor of the heat wave frequency over Western Europe at decadal time scales. Dong *et al.* (2017) allocate almost two thirds of the seasonal mean warming in Western European summers since the mid-1990s to changes in SST, while changes in greenhouse gases and anthropogenic aerosols form the remaining third. As the occurrence of warm and cold periods is strongly linked between our five study regions at decadal scales, changes in Atlantic SST have impacts to regions further east as well.

Knudsen *et al.* (2011) show that the current known mechanism of 55–70 year oscillations existed during most of the past 8,000 years. Hence, considering the AMO-effect on European summer temperatures alone, another 10–15 years of enhanced summer temperatures could follow in Europe, in case the current positive AMO phase will be as long as the previous. Afterwards, an AMO-related summer cooling could offset some of the anthropogenic effects in following decades. Such a transition may occur quite rapidly, like observed during the last transition from a warm to a cool AMO phase (Thompson *et al.*, 2010). Yet, despite the striking link between the AMO and European summer temperature variability since the 20th century such forecasts are speculative, since the physical mechanisms of the AMO and its links to European summer temperatures are not adequately understood. In addition, correlation values before the 20th century are much lower for unclear reasons, possibly related to inaccuracies in early measurements or unknown differences in the underlying physical mechanisms. In that context, recent research suggests a much smaller role of internal ocean dynamics than previously assumed, arguing that the AMO largely follows external forcing (i.e., anthropogenic warming and aerosol changes), and therefore may not be used as a predictor of future summer conditions (Haustein *et al.*, 2019). In any case, any decadal outlook of future summer temperatures is limited by the fact that the interplay of major teleconnection patterns and the role of oceanic circulation are just among a broad band of other contributors to the future of European summers.

4.3 | Seasonal supporting factors and anthropogenic effects on hot summers

This section summarizes the (currently known) additional natural drivers and the effects of global warming on occurrence and peculiarities of hot European summers. A positive feedback cycle of soil dryness, evaporation,

precipitation and temperature contributes to summer heat waves in Europe (Fischer *et al.*, 2007; Vautard *et al.*, 2007; Haarsma *et al.*, 2009; Quesada *et al.*, 2012). Soil moisture depletion directly in summer or previously during winter and spring, caused by precipitation deficits and/or warm temperatures, leads to reduced evaporation and latent cooling, causing a reduction in cloud cover, resulting in increasing solar energy at the surface and further soil drying, causing higher summer temperatures and so on (Seneviratne *et al.*, 2010). Dry (wet) Mediterranean winter and spring seasons cause a high (low) frequency of anomalously hot days during summer, often affecting other regions as well (Fischer *et al.*, 2007; Quesada *et al.*, 2012). Largest impacts are assumed for daily TX (Whan *et al.*, 2015). According to Fischer *et al.* (2007), moisture-temperature-interactions account for 50–80% of hot summer days in Europe. Soil desiccation in combination with atmospheric heat accumulation is believed to have played a relevant role for both the 2003 Western European as well as the 2010 Eastern European/Russian mega heat waves (Miralles *et al.*, 2014) and likely strongly contributed to the 2018 heat extremes as well.

Global warming plays indeed a major role in the observed and projected strong increase of heat conditions in Europe (IPCC, 2013; Christidis *et al.*, 2015; Haustein *et al.*, 2019). Continuously reduced aerosol emissions in combination with a reduction in cloudiness (‘solar brightening’) led to additional (specifically TX) temperature rises by increasing solar radiations at the surface since the 1980s (Wild, 2009; Tang *et al.*, 2012; Dong *et al.*, 2017). Further explanations reach above the background warming in Europe itself and include changes in atmospheric circulation patterns and blocking situations. A weakening atmospheric summer circulation over Europe is believed to contribute to more persistent and intensive heat waves, through a reduction in mean zonal wind speeds and an increase in quasi-stationary Rossby-waves because of the reduction in the Arctic-Tropics temperature gradient (Coumou *et al.*, 2015; Mann *et al.*, 2018). All aspects combined, researchers of the ‘world weather attribution project’ conclude that the probability of the 2018 summer heat wave in Scandinavia increased more than twofold compared to conditions without human contribution (WWA, 2018).

Further exacerbating heat conditions – involving previously discussed aspects – are expected by climate modellers within the 21st century in Europe. Those projections are based on large ensembles of regional climate model simulations from the EURO-CORDEX and ENSEMBLES projects. Lhotka *et al.* (2018) propose a doubling of Central European heat waves in the coming three decades (2020–2049 compared to 1970–1999), with (depending on the emission scenario) a much stronger intensification towards the end of the century. Similarly, Russo *et al.* (2015) conclude an

enhanced probability for ‘heatwaves comparable to or greater than the magnitude, extent and duration of the Russian heatwave in 2010’ within the next two decades (2021–2040). Likewise, Barriopedro *et al.* (2011) project a 5–10 time enhancement in probability for mega-heatwaves like 2003 and 2010 until 2050.

5 | SUMMARY AND CONCLUSIONS

We investigated the thermal characteristics of the 2018 summer, using a spatially well-distributed dataset of 67 European stations (west of ~30°E) with daily air temperature observations mainly starting already in the 19th or rarely even 18th century. Compiling such a long-term (secular), quality-optimized (homogenized) and complete dataset (low number of gaps) enabled us to robustly assess the extremeness of the 2018 summer in a secular time-perspective. Individual time series length was considered for analysing station extremes and creating continental maps, while European time series were presented for the period of 1855–2018 and records of five sub-regions considered from 1881 onwards.

The extreme long duration of the 2018 summer most clearly manifested itself in pronounced new continental maxima of SHY (April–September) temperature averages and the number of days with maxima over 20°C (WD) and 25°C (SU). Those three indices also reached new local maxima at more than half of our investigated stations. Records of other temperature indices, rather representing intense heat conditions, were particularly broken in the extended Baltic Sea region. Our data show that the accumulation of hot European summers since the 1990s is unprecedented within the instrumental past, in all our investigated five regions. Considering our 12 analysed indices, the extreme summer of 2003 still dominates the ranking of most indices, but it is now generally closely followed by 2018 (Table 3).

We show that a combination of long-term variations of teleconnection indices and the AMO, as well as seasonal and anthropogenic effects, supported both the recent hot summers and the extreme summer of 2018. Recent decades saw positive index values of EA and negative of EAWR and WP teleconnections. The AMO is in its positive (warm) phase since the 1990s. Global warming in combination with reduced aerosol emissions fostered higher temperatures. Feedback mechanisms between (increasing) soil dryness in the Mediterranean affect other regions as well via the impact of atmospheric circulation. The combination of all mentioned factors strongly supported the observed summer warming in Europe since the 1990s.

TABLE 3 Summary of five most extreme European summers for 12 index values

| Rank | SU _{av} | SHY _{av} | HW ₉₀ | HW ₉₅ | WD | SU | HD | TX ₉₀ | TX ₉₉ | TN | TN ₉₀ | TN ₉₉ |
|------|------------------|-------------------|------------------|------------------|-------------|-------------|-------------|------------------|------------------|-------------|------------------|------------------|
| 1 | 2003 | 2018 | 2018 | 2003 | 2018 | 2018 | 2003 | 2003 | 2015 | 2003 | 2003 | 2003 |
| 2 | 2018 | 2003 | 2003 | 2018 | 2006 | 2003 | 2015 | 2015 | 2003 | 2018 | 2018 | 2010 |
| 3 | 2015 | 2011 | 2006 | 2015 | 2014 | 1947 | 2018 | 2018 | 2012 | 2015 | 2010 | 2018 |
| 4 | 2017 | 2016 | 2015 | 2006 | 1947 | 2011 | 2012 | 2012 | 2010 | 2012 | 2015 | 2015 |
| 5 | 2006 | 2006 | 2010 | 2010 | 2011 | 2012 | 2017 | 1947 | 2007 | 2017 | 2006 | 2006 |

Note: Bold value shown in year 2018.

Finally, the observed and projected developments described in this paper point to continuing or rather increasing heat conditions in near-future European summers. The role of the AMO may introduce some uncertainties in the decades from 2030, possibly offsetting some of the projected warming. Yet, global warming will further accelerate. In any case, additional negative health impacts are expectable with continuing summer warming, spatially increasing from comparably low influences in northern towards very high impacts in southern Europe (Gasparrini *et al.*, 2017). Hence, a continuous monitoring of actual summer conditions and investigations of extraordinary events like 2018 is therefore necessary to (a) assess newly appearing extremes, (b) understand the underlying (new or known) mechanisms and (c) improve the interpretation of climate model outputs based on observed events.

ACKNOWLEDGEMENTS

A very special thank you goes to all the dedicated people at universities, national weather services and other institutions for their priceless efforts in data collection, digitalisation, processing and optimizing. Nowhere else is such abundant knowledge of metadata and station specifics gathered than locally. We also thank Antonello Squintu for his cooperativeness in sharing, discussing and optimizing the homogenized version of the ECA&D station data set. Finally, we thank Werner Partschefeld and Christoph Brendel for their technical support connected to data processing efforts.

ORCID

Andreas Hoy  <https://orcid.org/0000-0003-3733-6483>

ENDNOTES

¹The observed very warm May in region South-East was probably connected to the unprecedentedly warm April there (Section 3.1).

²Note that we only employed the NAO index after Li and Wang (Section 2.3) in this study. Other approaches with a specific focus on summery circulation conditions, like the summer-NAO of Folland *et al.* (2009), may yield different results.

REFERENCES

- Åström, D.O., Forsberg, B. and Rocklöv, J. (2011) Heat wave impact on morbidity and mortality in the elderly population: a review of recent studies. *Maturitas*, 69, 99–105.
- BAFU (Swiss Federal Ministry for Environment). (2018) *Niedrigwasser und hohe Wassertemperaturen im Sommer 2018*. Available at: <https://www.bafu.admin.ch/bafu/de/home/themen/wasser/dossiers/niedrigwasser-sommer-2018.html#1519731011> [Accessed 30th March 2020].
- Barriopedro, D., Fischer, E.M., Luterbacher, J., Trigo, R.M. and García-Herrera, R. (2011) The hot summer of 2010: redrawing the temperature record map of Europe. *Science*, 332(6026), 220–224. <https://doi.org/10.1126/science.1201224>.
- Baur, F. (1947) *Musterbeispiele Europäischer Großwetterlagen*. Wiesbaden: Dietrich'sche Verlagsbuchhandlung, p. 35.
- Beck, H.E., Zimmermann, N.E., McVicar, T.R., Verpogolan, N., Berg, A. and Wood, E.F. (2018) Present and future Köppen-Geiger climate classification maps at 1-km resolution. *Scientific Data*, 5, 180214. <https://doi.org/10.1038/sdata.2018.214>.
- Begert, M., Schlegel, T. and Kirchhofer, W. (2005) Homogeneous temperature and precipitation series of Switzerland from 1864 to 2000. *International Journal of Climatology*, 25, 65–80. <https://doi.org/10.1002/joc.1118>.
- BFG (German Federal Institute for Hydrology). (2019) *Das Niedrigwasser 2018*. Available at: https://doi.org/10.5675/BfG-Niedrigwasserbroschuere_2018 [Accessed 30th March 2020].
- BMEL (German Federal Ministry of Food and Agriculture). (2018) *Erntebericht 2018*. Available at: https://www.bmel.de/SharedDocs/Downloads/Landwirtschaft/Markt-Statistik/Ernte2018Bericht.pdf?__blob=publicationFile [Accessed 30th March 2020].
- BMEL (German Federal Ministry of Food and Agriculture). (2019). *Ergebnisse der Waldzustandserhebung 2018*. Available at: https://www.bmel.de/SharedDocs/Downloads/Broschueren/ErgebnisseWaldzustandserhebung2018.pdf?__blob=publicationFile [Accessed 30th March 2020].
- Böhm, R., Jones, P.D., Hiebl, J., Frank, D., Brunetti, M. and Maugeri, M. (2010) The early instrumental warm-bias: a solution for long central European temperature series 1760–2007. *Climatic Change*, 101(1–2), 41–67. <https://doi.org/10.1007/s10584-009-9649-4>.
- Brandsma, T. (2016) *Homogenization of Daily Temperature Data of the Five Principal Stations in The Netherlands*. Technical report TR-356. 40 pp.
- Bueh, C. and Nakamura, H. (2007) Scandinavian pattern and its climatic impact. *Quarterly Journal of the Royal Meteorological Society*, 133(629), 2117–2131. <https://doi.org/10.1002/qj.173>.

- Burt, T. and Burt, S. (2019) *Oxford Weather and Climate Since 1767*. Oxford: Oxford University Press, p. 544 ISBN 9780198834632.
- Busuoiuc, A., Dumitrescu, A., Soare, E. and Orzan, A. (2007) Summer anomalies in 2007 in the context of extremely hot and dry summers in Romania. *Romanian Journal of Meteorology*, 9 (1–2), 1–17.
- Butler, C.J., Garcia Suarez, A.M., Coughlin, A.D.S. and Morrell, C. (2005) Air temperatures at Armagh Observatory, Northern Ireland, from 1796 to 2002. *International Journal of Climatology*, 25, 1055–1079. <https://doi.org/10.1002/joc.1148>.
- Christidis, N., Jones, G.S. and Stott, P.A. (2015) Dramatically increasing chance of extremely hot summers since the 2003 European heatwave. *Nature Climate Change*, 5, 46–50. <https://doi.org/10.1038/nclimate2468>.
- Cioffi, F., Lall, U., Rus, E. and Krishnamurthy, C.K.B. (2015) Space-time structure of extreme precipitation in Europe over the last century. *International Journal of Climatology*, 35(8), 1749–1760. <https://doi.org/10.1002/joc.4116>.
- Corobov, R., Sheridan, S., Opopol, N. and Ebi, K. (2013) Heat-related mortality in Moldova: the summer of 2007. *International Journal of Climatology*, 33(11), 2551–2560. <https://doi.org/10.1002/joc.3610>.
- Coumou, D., Lehmann, J. and Beckmann, J. (2015) The weakening summer circulation in the northern hemisphere mid-latitudes. *Science*, 348(6232), 324–327. <https://doi.org/10.1126/science.1261768>.
- CPC (Climate Prediction Center). (2012) *Northern Hemisphere Teleconnection Patterns*. Available at: <https://www.cpc.ncep.noaa.gov/data/teledoc/telecontents.shtml> [Accessed 30th March 2020].
- Della-Marta, P.M., Luterbacher, J., von Weissenfluh, H., Xoplaki, E., Brunet, M. and Wanner, H. (2007) Summer heat waves over Western Europe 1880–2003, their relationship to large-scale forcings and predictability. *Climate Dynamics*, 29 (2–3), 251–275. <https://doi.org/10.1007/s00382-007-0233-1>.
- Demaree, G.R., Lachaert, P.J., Verhoeve, T. and Thoen, E. (2002) The long-term daily Central Belgium temperature (CBT) series (1767–1998) and early instrumental meteorological observations in Belgium. *Climatic Change*, 53(1–3), 269–293. <https://doi.org/10.1023/A:1014931211466>.
- Dole, R., Hoerling, M., Perlwitz, J., Eischeid, J., Pegion, P., Zhang, T., Quan, X.-W., Xu, T. and Murray, D. (2011) Was there a basis for anticipating the 2010 Russian heat wave? *Geophysical Research Letters*, 38(6), L06702. <https://doi.org/10.1029/2010GL046582>.
- Dong, B., Sutton, R.T. and Shaffrey, L. (2017) Understanding the rapid summer warming and changes in temperature extremes since the mid-1990s over Western Europe. *Climate Dynamics*, 48, 1537–1554. <https://doi.org/10.1007/s00382-016-3158-8>.
- Duchez, A., Frajka-Williams, E., Josey, S.A., Evans, D.G., Grist, J.P., Marsh, R., McCarthy, G.D., Sinha, B., Berry, D.I. and Hirschi, J. J.M. (2016) Drivers of exceptionally cold North Atlantic Ocean temperatures and their link to the 2015 European heat wave. *Environmental Research Letters*, 11, 074004. <https://doi.org/10.1088/1748-9326/11/7/074004>.
- DWD (German Weather Service). (2018a) *Vorläufiger Rückblick auf den Sommer 2018 – eine Bilanz extremer Wetterereignisse*. Available at: https://www.dwd.de/DE/leistungen/besondereereignisse/temperatur/20180803_bericht_sommer2018.pdf?__blob=publicationFile&v=5 [Accessed 30th March 2020].
- DWD (German Weather Service). (2018b) *2018 wärmster Sommer im Norden und Osten Deutschlands*. Available at: https://www.dwd.de/DE/leistungen/besondereereignisse/temperatur/20180906_waermstersommer_nordenosten2018.pdf?__blob=publicationFile&v=7 [Accessed 30th March 2020].
- DWD (German Weather Service). (2019a) *Deutschlandwetter im Juli 2019*. Available at: https://www.dwd.de/DE/presse/pressemitteilungen/DE/2019/20190730_deutschlandwetter_juli_news.html?nn=495078 [Accessed 30th March 2020].
- DWD (German Weather Service). (2019b) *Großwetterlagenklassifikation 2003–2019*. Available at: <https://www.dwd.de/DE/leistungen/grosswetterlage/grosswetterlage.html> [Accessed 30th March 2020].
- ECA&D (European Climate Assessment & Dataset). (2013) *Algorithm Theoretical Basis Document (ATBD), version 10.7*. Royal Netherlands Meteorological Institute KNMI, 47 pp.
- EMHI (Estonian Meteorological and Hydrological Institute). (2018) *Keskmisest kuivema, soojema ja päikesepaistelisema suve ülevaade*. Available at: <http://www.ilmateenistus.ee/2018/09/keskmisest-kuivema-soojema-ja-paikesepaistelisema-suve-ulevaade/> [Accessed 30th March 2020].
- Enfield, D.B., Mestas-Nuñez, A.M. and Trimble, P.J. (2001) The Atlantic multidecadal oscillation and its relation to rainfall and river flows in the continental U.S. *Geophysical Research Letters*, 28(10), 2077–2080. <https://doi.org/10.1029/2000GL012745>.
- Fischer, E.M., Seneviratne, S.I., Lüthi, D. and Schär, C. (2007) Contribution of land-atmosphere coupling to recent European summer heat waves. *Geophysical Research Letters*, 34(6), L06707. <https://doi.org/10.1029/2006GL029068>.
- FMI (Finish Meteorological Institute). (2018) *The Summer from May to August was Warmer Than Ever in Recorded History*. Available at: <https://en.ilmatieltenlaitos.fi/press-release/656561883> [Accessed 30th March 2020].
- Folland, C.K., Knight, J., Linderholm, H.W., Fereday, D., Ineson, S. and Hurrell, J.W. (2009) The summer North Atlantic oscillation: past, present, and future. *Journal of Climate*, 22, 1082–1103. <https://doi.org/10.1175/2008JCLI2459.1>.
- Founda, D. and Giannakopoulos, C. (2009) The exceptionally hot summer of 2007 in Athens, Greece – a typical summer in the future climate? *Global and Planetary Change*, 67(3–4), 227–236.
- Gasparrini, A., Guo, Y., Sera, F., Vicedo-Cabrera, A.M., Huber, V., Tong, S., de Sousa Zanotti Stagliorio Coelho, M., Nascimento Saldiva, P.H., Lavigne, E., Matus Correa, P., Valdes Ortega, N., Kan, H., Osorio, S., Kyselý, J., Urban, A., Jaakkola, J.J.K., Rytty, N.R.I., Pascal, M., Goodman, P.G., Zeka, A., Michelozzi, P., Scortichini, M., Hashizume, M., Honda, Y., Hurtado-Diaz, M., Cesar Cruz, J., Seposo, X., Kim, H., Tobias, A., Iñiguez, C., Forsberg, B., Åström, D.O., Ragetti, M. S., Guo, Y.L., Wu, C.F., Zanobetti, A., Schwartz, J., Bell, M.L., Dang, T.N., van, D.D., Heaviside, C., Vardoulakis, S., Hajat, S., Haines, A. and Armstrong, B. (2017) Projections of temperature-related excess mortality under climate change scenarios. *The Lancet Planetary Health*, 1(9), 360–367. [https://doi.org/10.1016/S2542-5196\(17\)30156-0](https://doi.org/10.1016/S2542-5196(17)30156-0).
- Haarsma, R.J., Selten, F., vd Hurk, B., Hazeleger, W. and Wang, X. (2009) Drier Mediterranean soils due to greenhouse warming bring easterly winds over summertime Central Europe.

- Geophysical Research Letters*, 36, L04705. <https://doi.org/10.1029/2008GL036617>.
- Hauser, M., Orth, R. and Seneviratne, S.I. (2016) Role of soil moisture versus recent climate change for the 2010 heat wave in Western Russia. *Geophysical Research Letters*, 43, 2819–2826. <https://doi.org/10.1002/2016GL068036>.
- Haustein, K., Otto, F.E.L., Venema, V., Jacobs, P., Cowtan, K., Hausfather, Z., Way, R.G., White, B., Subramanian, A. and Schurer, A.P. (2019) A limited role for unforced internal variability in twentieth-century warming. *Journal of Climate*, 32, 4893–4917. <https://doi.org/10.1175/JCLI-D-18-0555.1>.
- Hess, P. and Brezowsky, H. (1977) *Katalog der Großwetterlagen Europas*, Vol. 15/113, 3rd edition. Offenbach: Ber Dt Wetterd, p. 68.
- Holtanová, E., Valerianová, A., Crhová, L. and Racko, S. (2015) Heat wave of August 2012 in The Czech Republic: comparison of two approaches to assess high temperature event. *Studia Geophysica et Geodaetica*, 59(1), 159–172. <https://doi.org/10.1007/s11200-014-0805-6>.
- Hoy, A., Hänsel, S., Skalák, P., Ustrnul, Z. and Bochníček, O. (2017) The extreme European summer of 2015 in a long-term perspective. *International Journal of Climatology*, 37(2), 943–962. <https://doi.org/10.1002/joc.4751>.
- Hoy, A., Jaagus, J., Sepp, M. and Matschullat, J. (2013a) Spatial response of two European atmospheric circulation classifications (data from 1901 to 2010). *Theoretical and Applied Climatology*, 112(1–2), 73–88. <https://doi.org/10.1007/s00704-012-0707-x>.
- Hoy, A., Sepp, M. and Matschullat, J. (2013b) Atmospheric circulation variability in Europe and northern Asia (1901 to 2010). *Theoretical and Applied Climatology*, 113(1–2), 105–126. <https://doi.org/10.1007/s00704-012-0770-3>.
- Hoy, A., Sepp, M. and Matschullat, J. (2013c) Large-scale atmospheric circulation forms and their impact on air temperature in Europe and northern Asia. *Theoretical and Applied Climatology*, 113(3–4), 643–658. <https://doi.org/10.1007/s00704-012-0813-9>.
- Hurrell, J.W. (1995) Decadal trends in the North Atlantic oscillation: regional temperatures and precipitation. *Science*, 296, 676–679.
- Huth, R. (2010) Synoptic-climatological applicability of circulation classifications from the COST733 collection: first results. *Physics and Chemistry of the Earth*, 35, 388–394.
- IPCC. (2013) Climate change 2013: the physical science basis. In: Stocker, T.F., Qin, D., Plattner, G.-K., Tignor, M., Allen, S.K., Boschung, J., Nauels, A., Xia, Y., Bex, V. and Midgley, P.M. (Eds.) *Contribution of Working Group I to the Fifth Assessment Report of the Intergovernmental Panel on Climate Change*. Cambridge, United Kingdom and New York, NY, USA: Cambridge University Press.
- ISPRA (Istituto Superiore per la Protezione e la Ricerca Ambientale). (2018) *Gli indicatori del clima in Italia nel 2018*. Stato dell'Ambiente 88/2019. 76 pp. ISBN 978-88-448-0955-3.
- James, P.M. (2007) An objective classification method for Hess and Brezowsky Grosswetterlagen over Europe. *Theoretical and Applied Climatology*, 88(1–2), 17–42. <https://doi.org/10.1007/s00704-006-0239-3>.
- Jones, P.D. and Lister, D.H. (2002) The daily temperature record for St. Petersburg (1743–1996). *Climatic Change*, 53(1–3), 253–267. <https://doi.org/10.1023/A:1014918808741>.
- Jones, P.D. and Lister, D.H. (2009) The influence of the circulation on surface temperature and precipitation patterns over Europe. *Climate of the Past*, 5, 259–267. <https://doi.org/10.5194/cp-5-259-2009>.
- JRC (Joint Research Centre of the European Commission). (2018) *Crop Monitoring in Europe, September 2018*. Available at: https://ec.europa.eu/info/sites/info/files/food-farming-fisheries/farming/documents/short-term-outlook-autumn-2018_en.pdf [Accessed 30th March 2020].
- Kaplan, A., Cane, M.A., Kushnir, Y., Clement, A.C., Blumenthal, M.B. and Rajagopalan, B. (1998) Analyses of global sea surface temperature 1856–1991. *Journal of Geophysical Research: Oceans*, 103(C9), 18567–18589. <https://doi.org/10.1029/97JC01736>.
- Kenworthy, J.M., Burt, T.P. and Cox, N.J. (2007) Durham University Observatory and its meteorological record. *Weather*, 62(10), 265–269. <https://doi.org/10.1002/wea.86>.
- Kew, S.F., Sjoukje, Y.F., van Oldenborgh, G.J., Otto, F.E.L., Vautard, R. and van der Schrier, G. (2019) The exceptional summer heat wave in Southern Europe 2017. *Bulletin of the American Meteorological Society*, 100(1), 49–53. <https://doi.org/10.1175/BAMS-D-18-0109.1>.
- Klein Tank, A.M., Zwiers, F.W. and Zhang, X. (2009) *Guidelines on Analysis of Extremes in a Changing Climate in Support of Informed Decisions for Adaptation*. Geneva: WMO.
- KMI (Meteorological Institute of Belgium). (2019) *Juli 2019: absolute warmterecord gebroken*. Available at: <https://www.meteo.be/nl/info/nieuwsoverzicht/juli-2019-absolute-warmterecord-gebroken> [Accessed 30th March 2020].
- Knight, J.R., Allan, R.J., Folland, C.K., Vellinga, M. and Mann, M. E. (2005) A signature of persistent natural thermohaline circulation cycles in observed climate. *Geophysical Research Letters*, 32(20), L20708. <https://doi.org/10.1029/2005GL024233>.
- Knight, J.R., Folland, C.K. and Scaife, A.A. (2006) Climate impacts of the Atlantic multidecadal oscillation. *Geophysical Research Letters*, 33(17), LT17706. <https://doi.org/10.1029/2006GL026242>.
- KNMI (Meteorological Institute of the Netherlands). (2018) *Warmste zomer in drie eeuwen*. Available at: <https://www.knmi.nl/over-het-knmi/nieuws/warmste-zomer-in-drie-eeuwen> [Accessed 30th March 2020].
- KNMI (Meteorological Institute of the Netherlands). (2019) *Temperatuur door historische grens van 40°C*. Available at: <https://www.knmi.nl/over-het-knmi/nieuws/temperatuur-door-historische-grens-van-40-c> [Accessed 30th March 2020].
- Knudsen, M.F., Seidenkrantz, M.S., Jacobsen, B.H. and Kujpers, A. (2011) Tracking the Atlantic multidecadal oscillation through the last 8,000 years. *Nature Communications*, 2(178), 178. <https://doi.org/10.1038/ncomms1186>.
- Kornhuber, K., Osprey, S., Coumou, D., Petri, S., Petoukhov, V., Rahmstorf, S. and Gray, L. (2019) Extreme weather events in early summer 2018 connected by a recurrent hemispheric wave-7 pattern. *Environmental Research Letters*, 14(5), 054002. <https://doi.org/10.1088/1748-9326/ab13bf>.
- Kożuchowski, K., Trepinańska, J. and Wibig, J. (1994) The air temperature in Cracow from 1826 to 1990: persistence, fluctuations and the urban effect. *International Journal of Climatology*, 14(9), 1035–1049. <https://doi.org/10.1002/joc.3370140908>.

- Krisinformation (Emergency Information of Swedish Authorities). (2018) *In English About the Forest Fires*. Available at: <https://www.krisinformation.se/detta-kan-handa/handelser-och-storningar/2018/brandrisk2018/in-english-about-the-forest-fires> [Accessed 30th March 2020].
- Krzyżewska, A. and Dyer, J. (2018) The August 2015 megahotwave in Poland in the context of past events. *Weather*, 73 (7), 207–214. <https://doi.org/10.1002/wea.3244>.
- Kysely, J. (2002) Temporal fluctuations in heat waves at Prague–Klementinum, The Czech Republic, from 1901–97, and their relationships to atmospheric circulation. *International Journal of Climatology*, 22(1), 33–50. <https://doi.org/10.1002/joc.720>.
- Kysely, J. (2010) Recent severe heat waves in Central Europe: how to view them in a long-term prospect? *International Journal of Climatology*, 30(1), 89–109. <https://doi.org/10.1002/joc.1874>.
- Lhotka, O. and Kysely, J. (2015a) Characterizing joint effects of spatial extent, temperature magnitude and duration of heat waves and cold spells over Central Europe. *International Journal of Climatology*, 35(7), 1232–1244. <https://doi.org/10.1002/joc.4050>.
- Lhotka, O. and Kysely, J. (2015b) Hot Central-European summer of 2013 in a long-term context. *International Journal of Climatology*, 35, 4399–4407. <https://doi.org/10.1002/joc.4277>.
- Lhotka, O., Kysely, J. and Farda, A. (2018) Climate change scenarios of heat waves in Central Europe and their uncertainties. *Theoretical and Applied Climatology*, 131(3–4), 1043–1054. <https://doi.org/10.1007/s00704-016-2031-3>.
- Li, J. and Wang, J. (2003) A new North Atlantic oscillation index and its variability. *Advances in Atmospheric Sciences*, 20(5), 661–676. <https://doi.org/10.1007/BF02915394>.
- Li, M., Shaohua, G., Bi, P., Yang, J. and Liu, Q. (2015) Heat waves and morbidity: current knowledge and further direction – a comprehensive literature review. *International Journal of Environmental Research and Public Health*, 12(5), 5256–5283. <https://doi.org/10.3390/ijerph120505256>.
- Lundstad, E. and Tveito, O.E. (2016) *Homogenisation of daily mean temperature in Norway*. MET report 6/2016. 78 pp. ISSN 2387-4201.
- Luterbacher, J., Dietrich, D., Xoplaki, E., Grosjean, M. and Wanner, H. (2004) European seasonal and annual temperature variability, trends, and extremes since 1500. *Science (New York, NY)*, 303(5663), 1499–1503. <https://doi.org/10.1126/science.1093877>.
- Mann, M.E., Rahmstorf, S., Kornhuber, K., Steinmann, B.A., Miller, S.K., Petri, S. and Coumou, D. (2018) Projected changes in persistent extreme summer weather events: the role of quasi-resonant amplification. *Science Advances*, 4(10), eaat3272. <https://doi.org/10.1126/sciadv.aat3272>.
- Manning, C., Widmann, M., Bevacqua, E., van Loon, A.F., Maraun, D. and Vrac, M. (2019) Increased probability of compound long-duration dry & hot events in Europe during summer (1950–2013). *Environmental Research Letters*, 14, 094006. <https://doi.org/10.1088/1748-9326/ab23bf>.
- Maugeri, M., Buffoni, L. and Chlistovsky, F. (2002a) Daily Milan temperature and pressure series (1763–1998): history of the observations and data and metadata recovery. *Climatic Change*, 53, 101–117. <https://doi.org/10.1023/A:1014923027396>.
- Maugeri, M., Buffoni, L., Delmonte, B. and Fassina, A. (2002b) Daily Milan temperature and pressure series (1763–1998): completing and homogenising the data. *Climatic Change*, 53, 119–149. <https://doi.org/10.1023/A:1014923027396>.
- MeteoFrance. (2019) *Record absolu de chaleur battu: 45,9 °C dans le Gard, du jamais vu en France*. Available at: <http://www.meteofrance.fr/actualites/73726667-record-absolu-de-chaleur-battu-45-9-c-dans-le-gard-du-jamais-vu-en-france> [Accessed 30th March 2020].
- MeteoSwiss. (2018) *Extreme Regenarmut und Rekordwärme*. Available at: <https://www.meteoschweiz.admin.ch/home.subpage.html/de/data/blogs/2018/7/extreme-regenarmut-und-rekordwaerme.html> [Accessed 30th March 2020].
- MetOffice. (2018) *Was Summer 2018 the Hottest on Record?* Available at: <https://www.metoffice.gov.uk/about-us/press-office/news/weather-and-climate/2018/end-of-summer-stats> [Accessed 30th March 2020].
- Miralles, D.G., Teuling, A.J., van Heerwaarden, C.C. and Vilà-Guerau de Arellano, J. (2014) Mega-heatwave temperatures due to combined soil desiccation and atmospheric heat accumulation. *Nature Geoscience*, 7, 345–349. <https://doi.org/10.1038/ngeo2141>.
- Moberg, A., Alexandersson, H., Bergström, H. and Jones, P.D. (2003) Were Southern Swedish summer temperatures before 1860 as warm as measured? *International Journal of Climatology*, 23, 1495–1521. <https://doi.org/10.1002/joc.945>.
- Moberg, A., Bergström, H., Ruiz Krigsman, J. and Svanered, O. (2002) Daily air temperature and pressure series for Stockholm (1756–1998). *Climatic Change*, 53, 171–212. <https://doi.org/10.1023/A:1014966724670>.
- Moore, G.W.K. and Renfrew, I.A. (2012) Cold European winters: interplay between the NAO and the East Atlantic mode. *Atmospheric Science Letters*, 13(1), 1–8. <https://doi.org/10.1002/asl.356>.
- NATO. (2018) *Forest Fires in Sweden*. Available at: https://www.nato.int/cps/en/natohq/news_157546.htm [Accessed 30th March 2020].
- Otto, F.E.L., Massey, N., van Oldenbourgh, G.J., Jones, R.G. and Allen, M.R. (2012) Reconciling two approaches to attribution of the 2010 Russian heat wave. *Geophysical Research Letters*, 39, L04702. <https://doi.org/10.1029/2011GL050422>.
- Parker, D.E. and Horton, B.E. (2005) Uncertainties in the Central England temperature series 1878–2003 and some improvements to the maximum and minimum series. *International Journal of Climatology*, 25, 1173–1188. <https://doi.org/10.1002/joc.1190>.
- Quesada, B., Vautard, R., Yiou, P., Hirschi, M. and Seneviratne, S.I. (2012) Asymmetric European summer heat predictability from wet and dry southern winters and springs. *Nature Climate Change*, 2, 736–741. <https://doi.org/10.1038/nclimate1536>.
- Rahmstorf, S. and Coumou, D. (2011) Increase of extreme events in a warming world. *Proceedings of the National Academy of Sciences*, 108(44), 17905–17909. <https://doi.org/10.1073/pnas.1101766108>.
- Rebetez, M., Dupont, O. and Giroud, M. (2009) An analysis of the July 2006 heatwave extent in Europe compared to the record year of 2003. *Theoretical and Applied Climatology*, 95(1–2), 1–7. <https://doi.org/10.1007/s00704-007-0370-9>.
- Robine, J.M., Cheung, S.L., Le Roy, S., van Oyen, H. and Herrmann, F.R. (2007) *Report on Excess Mortality in Europe during Summer 2003. EU Community Action Programme for Public Health*. Brussels, Belgium: European Commission, p. 2007.

- Russo, S., Dosio, A., Graversen, R.G., Sillmann, J., Carrao, H., Dunbar, M.B., Singleton, A., Montagna, P., Barbola, P. and Vogt, J.V. (2014) Magnitude of extreme heat waves in present climate and their projection in a warming world. *JGR Atmospheres*, 119(22), 12500–12512. <https://doi.org/10.1002/2014JD022098>.
- Russo, S., Sillmann, J. and Fischer, E.M. (2015) Top ten European heatwaves since 1950 and their occurrence in the coming decades. *Environmental Research Letters*, 10 (12), 124003. <https://doi.org/10.1088/1748-9326/10/12/124003>.
- Rust, H.W., Richling, A., Bissolli, P. and Ulbrich, U. (2015) Linking teleconnection patterns to European temperature – a multiple linear regression model. *Meteorologische Zeitschrift*, 24, 411–423. <https://doi.org/10.1127/metz/2015/0642>.
- Sánchez-Benítez, A., García-Herrera, R., Barriopedro, D., Sousa, P. M. and Trigo, R.M. (2018) June 2017: the earliest European summer mega-heatwave of reanalysis period. *Geophysical Research Letters*, 45(4), 1955–1962. <https://doi.org/10.1002/2018GL077253>.
- Schär, C., Vidale, P.L., Lüthi, D., Frei, C., Häberli, C., Liniger, M.A. and Appenzeller, C. (2004) The role of increasing temperature variability in European summer heatwaves. *Nature*, 427(6972), 332–336. <https://doi.org/10.1038/nature02300>.
- Seneviratne, S.I., Corti, T., Davin, E.L., Mirschi, M., Jaeger, E.B., Lehner, I., Orlowsky, B. and Teuling, A.J. (2010) Investigating soil moisture–climate interactions in a changing climate: a review. *Earth-Science Reviews*, 99, 125–161. <https://doi.org/10.1016/j.earscirev.2010.02.004>.
- Shevchenko, O., Lee, H., Snizhko, S. and Mayer, H. (2014) Long-term analysis of heat waves in Ukraine. *International Journal of Climatology*, 34(5), 1642–1650. <https://doi.org/10.1002/joc.3792>.
- SHMI (Swedish Meteorological and Hydrological Institute). (2018) *Sommaren 2018 – Extremt varm och solig*. Available at: <https://www.smhi.se/klimat/klimatet-da-och-nu/arets-vader/sommaren-2018-extremt-varm-och-solig-1.138134> [Accessed 30th March 2020].
- Simolo, C., Brunetti, M., Maugeri, M. and Nanni, T. (2014) Increasingly warm summers in the Euro–Mediterranean zone: mean temperatures and extremes. *Regional Environmental Change*, 14(5), 1825–1832. <https://doi.org/10.1007/s10113-012-0373-7>.
- Squintu, A.A., van der Schrier, G., Brugnara, Y. and Klein, T.A. (2019) Homogenization of daily temperature series in the European climate Assessment & Dataset. *International Journal of Climatology*, 39(3), 1243–1261. <https://doi.org/10.1002/joc.5874>.
- Sutton, R.T. and Dong, B. (2012) Atlantic Ocean influence on a shift in European climate in the 1990s. *Nature Geoscience*, 5, 788–792. <https://doi.org/10.1038/ngeo1595>.
- Sutton, R.T. and Hodson, D.L.R. (2005) Atlantic Ocean forcing of north American and European summer climate. *Science*, 309 (5731), 115–118. <https://doi.org/10.1126/science.1109496>.
- Tang, Q., Leng, G. and Groisman, P.Y. (2012) European hot summers associated with a reduction of cloudiness. *Journal of Climate*, 25, 3637–3644. <https://doi.org/10.1175/JCLI-D-12-00040.1>.
- Thompson, D.W.J., Wallace, J.M., Kennedy, J.J. and Jones, P.D. (2010) An abrupt drop in Northern Hemisphere Sea surface temperature around 1970. *Nature*, 467, 444–447. <https://doi.org/10.1038/nature09394>.
- Thompson, R. (1995) Complex demodulation and the estimation of the changing continentality of Europe's climate. *International Journal of Climatology*, 15(2), 175–185. <https://doi.org/10.1002/joc.3370150204>.
- Trenberth, K.E. and Fasullo, J.T. (2012) Climate extremes and climate change: the Russian heat wave and other climate extremes of 2010. *Journal of Geophysical Research*, 117, D17103. <https://doi.org/10.1029/2012JD018020>.
- Unkašević, M. and Tošić, I. (2011) The maximum temperatures and heat waves in Serbia during the summer of 2007. *Climatic Change*, 108(1–2), 207–223. <https://doi.org/10.1007/s10584-010-0006-4>.
- van den Besselaar, E.J.M., Klein Tank, A.M.G. and van der Schrier, G. (2010) Influence of circulation types on temperature extremes in Europe. *Theoretical and Applied Climatology*, 99, 431–439. <https://doi.org/10.1007/s00704-009-0153-6>.
- Vautard, R., Yiou, P., Andrea, F.D., de Noblet, N., Viovy, N., Cassou, C., Polcher, J., Ciais, P., Kageyama, M. and Fan, Y. (2007) Summertime European heat and drought waves induced by wintertime Mediterranean rainfall deficit. *Geophysical Research Letters*, 34, L07711. <https://doi.org/10.1029/2006GL028001>.
- Werner, P.C. and Gerstengarbe, F.-W. (2010) *Katalog der Großwetterlagen Europas (1881–2009) nach Paul Hess und Helmut Brezowsky*. Potsdam: Potsdam Institute for Climate Change Impact Research.
- Whan, K., Zscheischler, J., Orth, R., Shongwe, M., Rahimi, M., Asare, E.O. and Seneviratne, S.I. (2015) Impact of soil moisture on extreme maximum temperatures in Europe. *Weather and Climate Extremes*, 9, 57–67. <https://doi.org/10.1016/j.wace.2015.05.001>.
- Wijngaard, J.B., Klein Tank, A.M.G. and Können, G.P. (2003) Homogeneity of 20th century European daily temperature and precipitation series. *International Journal of Climatology*, 23(6), 679–692. <https://doi.org/10.1002/joc.906>.
- Wild, M. (2009) Global dimming and brightening: a review. *Journal of Geophysical Research*, 114, D00D16. <https://doi.org/10.1029/2008JD011470>.
- WWA (World Weather Attribution). (2018) *Heatwave in Northern Europe, Summer 2018*. Available at: <https://www.worldweatherattribution.org/attribution-of-the-2018-heat-in-northern-europe/> [Accessed 30th March 2020].
- ZAMG (Austrian Meteorological Institute). (2018) *Wärmstes Sommerhalbjahr der Messgeschichte*. Available at: <https://www.zamg.ac.at/cms/de/klima/news/waermstes-sommerhalbjahr-der-messgeschichte> [Accessed 30th March 2020].

SUPPORTING INFORMATION

Additional supporting information may be found online in the Supporting Information section at the end of this article.

How to cite this article: Hoy A, Hänsel S, Maugeri M. An endless summer: 2018 heat episodes in Europe in the context of secular temperature variability and change. *Int J Climatol*. 2020;1–22. <https://doi.org/10.1002/joc.6582>